

Corrosion Resistance of Bottom Ash and Fly Ash-Based Reinforced Geopolymer Concretes
Using Half Cell Potential and Linear Polarization Resistance Methods

Priyanka Morla

Bachelor of Engineering, Jawaharlal Nehru Technology University, 2013

A Report Submitted in Partial Fulfillment of
the Requirements for the Degree of

MASTER OF ENGINEERING

In the Department of Mechanical Engineering

© Priyanka Morla, 2018

University of Victoria

All rights reserved. This report may not be reproduced in whole or in part, by photocopy
or other means, without the permission of the author.

Supervisory Committee

The Corrosion Resistance of Bottom Ash and Fly Ash-Based Reinforced Geopolymer Concretes
Using Half Cell and Linear Polarization Resistance methods

by

Priyanka Morla

Bachelor of Engineering, Jawaharlal Nehru Technological University, 2013

Supervisory Committee

Dr. Rishi Gupta, **Supervisor**
Department of Civil Engineering

Dr. Caterina Valeo, **Supervisor**
Department of Mechanical Engineering

Abstract

The production of Portland cement causes environmental pollution due to the amount of carbon dioxide released into the atmosphere. This environmental pollution can be reduced by improving the usage of industrial by-products. Geopolymer is a new concept that does not involve the use of Portland cement as a binder. Geopolymer Concrete (GPC) is formed by using such by-products and produces concrete without using any Ordinary Portland Cement (OPC). It produces the concrete by mixing the Alumino–Silicate source materials such as fly ash or slag with alkali activators such as KOH or NaOH. Due to the wide availability and low cost, industrial waste residuals such as fly ash are commonly used as the source material for the manufacture of GPC. The durability of GPC should be calculated and compared to OPC in order to consider Geopolymer concrete as an alternative to OPC. To achieve this goal, 12 molar Geopolymer concrete and 40 MPa ordinary Portland cement concrete specimens were prepared and tested for corrosion rate. A combination of fly ash and bottom ash was used as the basic source material which is activated by geopolymerization process to be the concrete binder. Instead of using sodium based activators, the alkaline liquids used in this project for the process of polymerization are the solutions of potassium hydroxide (KOH) and potassium silicate (K_2SiO_3), due to its better contribution on workability and strength. The results have shown that geopolymer concrete exhibited a higher resistance to chloride-induced corrosion; with low corrosion rate and low mass loss percentage, compared to OPC concrete.

Nomenclature

GPC - Geopolymer concrete

OPC - Ordinary Portland cement/concrete

HCP - Half cell potential

LPR- Linear polarization resistance

SSD – Saturated Surface Dry

RC – Reinforced concrete

Table of Contents

Supervisory Committee	ii
Abstract	iii
Nomenclature.....	iv
Table of Contents.....	v
List of Tables	vii
List of Figures.....	vii
Acknowledgments	viii
Dedication	x
Chapter 1: Introduction.....	11
1.1. General	11
1.2. Scope of work	11
1.3. Arrangement of report.....	12
Chapter 2: Literature Review	13
2.1. Geopolymers	13
2.1.1. Geopolymer Chemistry.....	13
2.1.2. Source materials.....	16
2.1.3. Alkaline Activator	17
2.1.4. Geopolymer applications.....	18
2.2. Corrosion of steel in concrete	19
2.3. Corrosion of steel in GPC	21
2.4. Half Cell Potential (HCP) method	22
2.5. Linear polarization resistance	23
Chapter 3: Experimental setup.....	26
3.1. Materials	26
3.1.1. Precursor material.....	26
3.1.2. Aggregates	26
3.1.3. Alkali activator.....	27
3.1.4. Ordinary Portland cement.....	27
3.2. Preparation of Geopolymer and OPC concretes	28
3.3. Specimen preparation	29

3.4. Curing temperature and conditions	29
3.5. Compressive strength test	30
3.6. Experimental program	31
3.6.1. Test specimens	31
3.6.2. Testing apparatus and materials	31
3.6.3. Chloride solution	32
3.7. Accelerated reinforced corrosion	32
3.8. Test procedure	33
3.9. Half cell potential	35
3.10. Linear Polarization Resistance Test	36
3.11. Residual Flexural Load Test	37
Chapter 4: Experimental results and discussion	39
4.1. Compressive strength	39
4.2. Cracking behaviour of the beams	39
4.3. HCP analysis	40
4.4. LPR analysis	42
4.5. Residual Flexural Load	44
4.6. Mass loss measurements	45
Chapter 5: Conclusions	47
References	48
Appendix A: LPR data graph of the OPC and GPC beams	50

List of Tables

Table 1 Applications of Geopolymer.....	18
Table 2 Potential of cell vs probability of corrosion	23
Table 3 Typical corrosion rates from LPR measurement [24]	25
Table 4 Chemical Composition of fly ash and bottom ash	26
Table 5 Mix design of Geopolymer concrete.....	28
Table 6 Mix design of OPC concrete	28
Table 7 Compressive strength development of OPC and GPC beams.....	39
Table 8 Half cell potential test results	41
Table 9 Linear polarization resistance test results	43
Table 10 Residual Flexural Loads of all the beams	44
Table 11 Percentage of mass loss of reinforced rebar	46

List of Figures

Figure 1 Conceptual model of Geopolymerization [4]	15
Figure 2 Chloride attack of steel reinforcement through concrete [14]	19
Figure 3 Corrosion reaction of steel reinforcement [14].....	20
Figure 4 Linear Polarization Resistance Measurement Setup [23].....	24
Figure 5 Model diagram of beam mold	29
Figure 6 Forney's Compressive Strength Test Machine.....	30
Figure 7 Schematic diagram of beam specimen	31
Figure 8 Beam specimens immersed in a chloride solution	32
Figure 9 FDOT Accelerated corrosion test setup [29].....	33
Figure 10 Schematic of Accelerated Corrosion test setup	34
Figure 11 Experimental setup for Accelerated Corrosion test	35
Figure 12 Schematic of the Half-cell potential measurement setup.....	36
Figure 13 Gamry Potentiostat setup for LPR test	37
Figure 14 Specimens under center point loading test.....	38
Figure 15 OPC beam after 200 hours of test	40
Figure 16 GPC beam after 200 hours of test	40
Figure 17 Average HCP values of OPC and GPC Beams	41
Figure 18 LPR graphical data of OPC beams	42
Figure 19 LPR graphical data of GPC beams	43
Figure 20 Broken OPC and GPC Beams.....	45
Figure 21 LPR data graph of GPC 1	50
Figure 22 LPR data graph of GPC 2	51
Figure 23 LPR data graph of GPC 3	51
Figure 24 LPR data graph of OPC 1	52
Figure 25 LPR data graph of OPC 2	52
Figure 26 LPR data graph of OPC 3	53

Acknowledgments

I wish to express my deepest gratitude to my supervisor Dr. Rishi Gupta. His support and consistent guidance made it possible for me to work on a topic that was of my interest. It was a great honor to finish this work under his supervision.

I am grateful to my co-supervisor Dr. Caterina Valeo for being an excellent guide. Thank you for encouraging and supporting me all the time.

I would like to thank Mr. Peyman Azarsa for sharing his knowledge and helping me with the mix design and casting work. I would like to thank Mr. Pejman Azarsa for helping me with the experimental setup, which would not have been possible to conduct on my own.

I would also like to thank Dr. Armando Tura and Mr. Mathew Walker for facilitating the research activities and providing with the materials needed in the lab.

Finally, I would like to acknowledge the love and unconditional support of my family and friends. I'd like to give special thanks to Renu Prasad Jetty for all his love and support.

Dedication

This work is dedicated to my beloved parents Krishnaiah Morla, Prasanna Morla and my fiancé Renu Prasad Jetty who have always been constant source of support in every possible way and encouragement throughout my life.

Chapter 1: Introduction

1.1. General

Geopolymer concrete made up of fly ash, bottom ash, coarse aggregate, fine sand, and an alkaline solution of potassium hydroxide and potassium silicate can play a vital role in its environmental control of CO₂ emissions. Steel reinforcement which is used in concrete structures has both advantages and disadvantages. It has a high compressive strength compared to other building materials; but also reduces the durability and longevity of concrete, due to its proneness to corrosion. The durability of concrete has a direct impact on its service behaviour, design life, and safety.

There are several factors that are responsible for degradation/deterioration in reinforced concrete structures. One of the factors responsible for the degradation is the corrosion of steel. The corrosion of steel reinforcement is complex. In simple words, it is similar to the electrochemical reaction of a battery. There are two stages of steel corrosion in concrete. In the first stage, the elements such as carbon dioxide or chloride present in the surrounding medium penetrate in concrete. In the second stage, these elements are in high concentration at the reinforcement level, resulting in rust growth, which can cause concrete cracking [1]. There are many techniques available for the prevention of corrosion in reinforced concrete structures. An Epoxy coating can prevent the formation of corrosion but can affect the rebar and concrete interface. Stainless steel reinforcement can also help to prevent the rust reaction, but cost is an issue. The cost of repairs can be minimized by delaying the corrosion cracking process.

1.2. Scope of work

Geopolymer concrete cylinders and beams were made to test the strength and corrosion durability and OPC cylinders and beams were made to test and compare the properties with GPC. In the beginning stage, cylinders were experimented to find the compressive strength to know about the properties of GPC at different ages. In the later stage, beams were experimented to study about the accelerated corrosion testing of centrally reinforced beams to find out the cracking behaviour of GPC after corrosion of the reinforcement. In the final step,

the beams were tested for the residual flexural strength of GPC and also to determine the mass loss of the reinforced steel.

1.3. Arrangement of report

This report starts with the chapter 2 which is the literature review on Geopolymers and their chemistry. It also gives a brief review on corrosion in GPC.

Chapter 3 describes the experimental set up carried out to develop the mix design, materials used, the mixing process and the preparation of GPC and OPC specimens. This chapter also describes the curing temperature and conditions of GPC. The tests performed to study the properties and behaviour of both OPC and GPC concretes.

Chapter 4 provides and discusses the test results.

Chapter 5 states the summary and conclusion of this project.

There is a list of references at the end of the report.

Chapter 2: Literature Review

2.1. Geopolymers

2.1.1. Geopolymer Chemistry

The concept of "GEOPOLYMER" was first proposed by Davidovits in the late 1970's [2]. He proposed that geopolymer is an alkaline liquid that could react with the aluminum (Al) and the silicon (Si) in a source or by-product materials such as fly ash to produce binders. In this case, the chemical reaction that takes place is known as polymerization process. He then introduced the term geopolymer to represent these binders. Geopolymers are chains or networks of mineral molecules connected with covalent bonds.

Davidovits suggested a word poly(sialate) to describe the chemical designation of geopolymers based on silico-aluminates. The term sialate is an abbreviation of silicon-oxo-aluminate. Poly(sialates) possess this empirical formula:

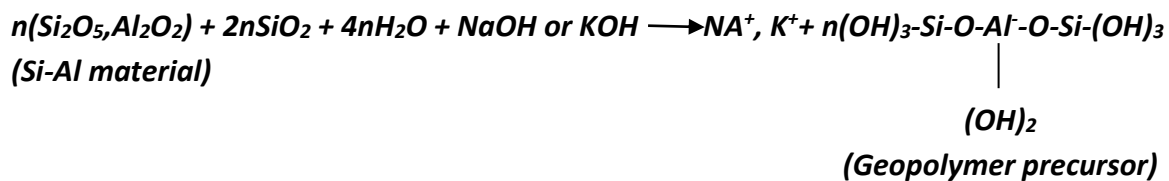


Where M = cation or the alkaline element such as potassium, calcium or sodium; n is a degree of polymerisation or polycondensation; the symbol – indicates the presence of a bond; z is 1,2,3, upto 32

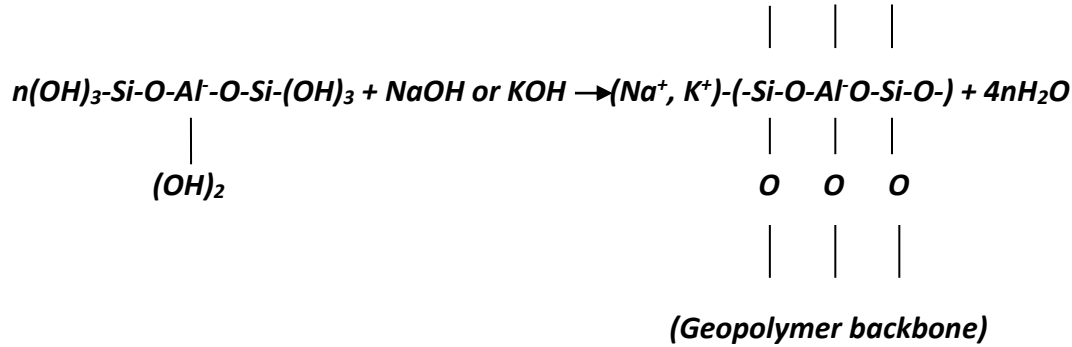
There are three types of silico-aluminate structures from polymerization reaction (Davidovits 1991),

- Poly(sialate), which has {-Si-O-Al-O-} as the repeating unit.
- Poly(sialate-siloxo), which has {-Si-O-Al-O-Si-O-} as the repeating unit.
- Poly(sialate-disiloxo), which has {-Si-O-Al-O-Si-O-Si-O-} as the repeating unit.

The following two stages chemical reactions represent the development of the geopolymer developed by Davidovits and are accepted widely:



(1)



(2)

Geopolymerization is a complicated process responsible for the formation of geopolymer. Geopolymer is formed when the alumino-silicate oxides (Si_2O_5 , Al_2O_2) chemically react with alkali polysilicates producing polymeric Si – O – Al – O bonds. Polysilicates are generally fine silica powder produced as a by-product of Ferro-silicon metallurgy or potassium or sodium silicate supplied by chemical Industries [3].

In the last reaction, we can see that water is released during the chemical reaction that occurs during the formation of geopolymers. Therefore, water plays no role in the chemical reaction. This is in contrast to the Portland cement concrete mixing during hydration process.

The general mechanism for alkali activation of alumino-silicates has been modeled by Gluhovsky by dividing the process into three stages: 1) destruction-coagulation; 2) coagulation-condensation; 3) condensation-crystallization [4]. Different authors have elaborated the Gluhovsky theory and applied the knowledge about zeolite synthesis to explain the geopolymerization process. Figure 1 shows a simple reaction mechanism for geopolymerization.

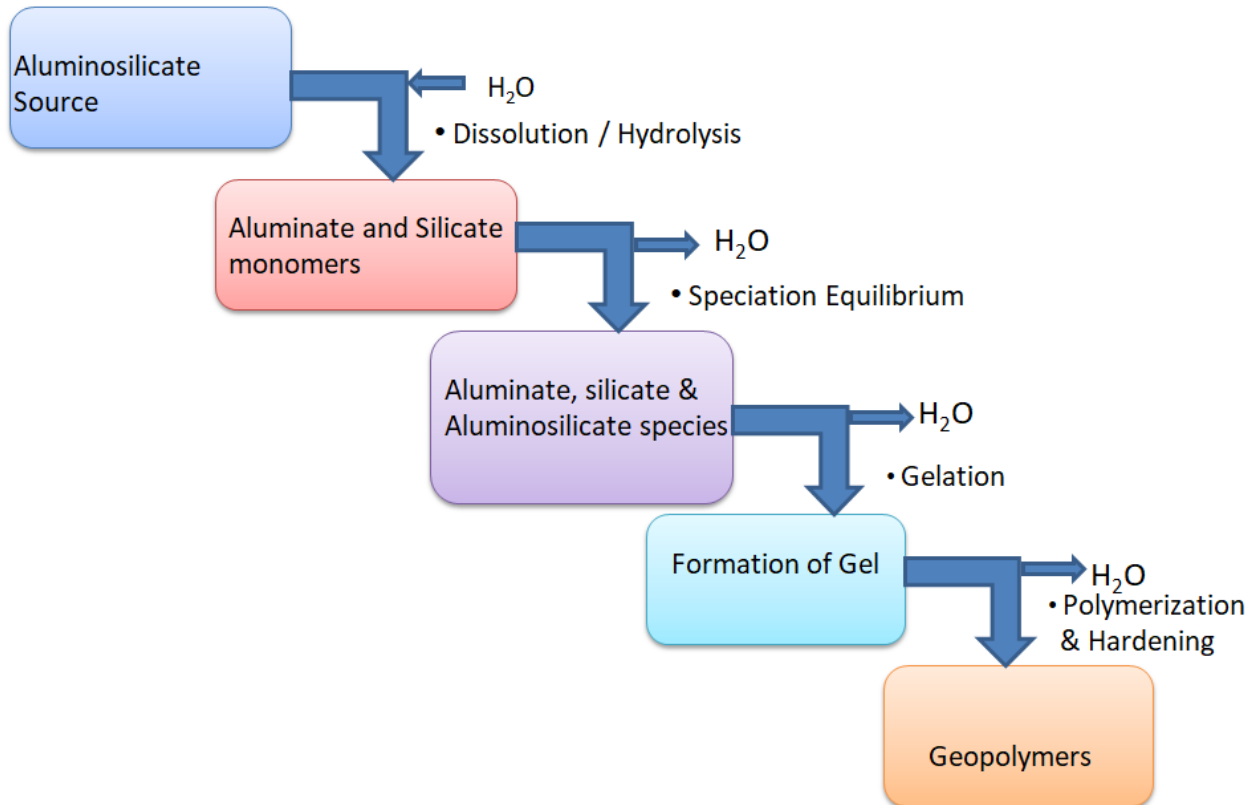


Figure 1 Conceptual model of Geopolymerization [4]

Dissolution of aluminosilicate source produces aluminate and silicate species by consuming the water. These species are incorporated into the aqueous phase, which contains silicate in the activating solution. The speciation equilibria within the solution containing aluminate, silicate and aluminosilicate species have been studied. This process releases water, which was consumed in the first step during dissolution. While water plays the role of a reaction medium, it stays within pores in the gel. After gelation, the system continues to reorganize, which will result in the three-dimensional aluminosilicate network, commonly accredited to geopolymers [4].

There are two main components of Geopolymers. They are source materials and the alkaline liquid. The materials that are rich in Silicon and Aluminum are used as source materials. The alkaline liquids are usually potassium or sodium based that are obtained from soluble alkali metals.

2.1.2. Source materials

Any material that is rich in Silicon and Aluminum in amorphous form can be considered as the possible source material for the manufacture of geopolymer. There are so many by-products available such as fly ash, slag, red mud, silica fume etc., could be considered as source materials. These source materials have been studied separately and in combined forms to produce geopolymer materials. The choice of source materials for making the geopolymer concretes depends upon the factors such as type of application, cost, availability and specific demands of the users.

FLY ASH

Fly ash is a by-product obtained in the process of production of coal from coal-fired power stations. Coal ash is a general term used to define the collection of residuals produced during the combustion of coal. Coal ash is further divided into two categories depending upon the particle size. Fly ash is the most voluminous and broadly known constituent. It occupies more than half of the coal leftovers and is the lightest kind of coal ash. They float on the exhaust stacks of the power plant. Bottom ash is the coarser component and occupies about 10 percent of the waste. Bottom ash doesn't float on to the exhaust stacks. It settles to the bottom of the boiler of the power plant [5].

Depending on the content of calcium, Fly ash is classified into two main types, namely ASTM class C and class F. Class F fly ash contains less than 7% lime (CaO). Whereas, Class C generally contains more than 20% lime. Class C is a self-cementing and does not require any activator. Class F requires a chemical activator such as sodium silicate or potassium silicate to form a geopolymer. The presence of calcium does not allow the formation of three dimensional polymeric network which results in a reduced final strength [6]. Class F is mostly used as a binder material in the projects since the curing process is performed at elevated temperatures.

Wallah and Rangan [7] conducted a study on fly ash based geopolymer concrete. For their study, they used low calcium (ASTM class F) dry fly ash obtained from a local coal burning power station. In this study they have described the long term properties of low-calcium fly ash based geopolymer concrete. They concluded that geopolymer possess excellent properties. Heat cured low calcium fly ash based geopolymer concrete has excellent compressive strength. It possesses excellent resistance to sulphate attack and also good acid resistance. They also

concluded that fly ash based geopolymer undergoes lesser creep compared to Portland cement concrete. It has very little drying shrinkage.

KAOLIN

Mustafa Al Bakri et al [8] performed microstructure studies on different types of geopolymer materials. In their research, they have used a locally supplied Kaolin which was of powder type with maximum 2% of moisture content. These researchers claim that the kaolin geopolymers contain pores that are predominantly in the meso pore size range, whereas the fly ash geopolymer contain pores that are predominantly in the micro pore size range. Kaolin based geopolymers possess sponge like amorphous gel indicating the structure experiences growth. In this case, the alkali activation is more effective. Kaolin contains more unreacted particles compared to fly ash. It is also studied that the kaolin based geopolymers have less dense structure compared to fly ash based geopolymer.

VOLCANIC ASH

Tchakoute et al [9] studied that volcanic ash can be used to produce geopolymer cements. The experiment used alkali fusion process to promote the dissolution of Si and Al from the volcanic ash and therefore to improve the reactivity of volcanic ash. This study showed that by improving the reactivity of volcanic ash by alkali fusion process and balancing the Na/Al through the addition of metakaolin, volcanic ashes can be used as a source material for the production of geopolymers.

2.1.3. Alkaline Activator

Alkaline activator is another important factor in the polymerization process. It is required for the dissolution of Al and Si from the source materials. The most commonly used alkaline liquid in geopolymerization is the combination of Sodium hydroxide (NaOH) with sodium silicate or potassium hydroxide (KOH) with potassium silicate.

In the most recent study by Wallah and Rangan [7], the long term properties of low-calcium fly ash based geopolymer concrete has been studied. Two different mixture proportions were formulated for making concrete specimens i.e. different amounts of sodium silicate and sodium hydroxide solution with molarities 8M and 14M. It was concluded that the solution with 8M possess high compressive strength.

2.1.4. Geopolymer applications

The first application of geopolymer was building products developed between 1973 and 1976. A fire resistant chip board panel was built comprised of a wooden core faced with two geopolymer nano composite coatings with one step manufacturing process [10].

Davidovits [11] has introduced a wide range of applications of geopolymer in industries such as aerospace and automobile, metallurgy and civil engineering and plastic industries. According to Davidovits [12] Some of the applications of geopolymers include: geopolymer cement and concrete, insulated panels and walls, fire resistant wood panels, low tech building materials, aluminum foundry application, refractory items, and aircraft interior

The type of application of geopolymeric materials is determined by the chemical structure in terms of the atomic ratio Si:Al in the polysialate. Davidovits proposed the possible applications of the geopolymer depending on the molar ratio of Si to Al, as given in table 1.

Table 1 Applications of Geopolymer

Si/Al	Application
1	Bricks, ceramics, fire protection
2	Low CO ₂ cements, concrete, radioactive and toxic waste encapsulation
3	Heat resistance composites, foundry equipment's, fibre glass composites
>3	Sealants for industry
20<Si/Al<35	Fire resistance and heat resistance fibre composites

A low ratio of Si:Al of 1, 2, or 3 initiates a 3D-Network that is very rigid, while Si:Al ratio higher than 15 provides a polymeric character to the geopolymeric material. It can be seen from Table 1 that for many applications in the civil engineering field a low Si:Al ratio is suitable.

Davidovits also explored the application of geopolymer in toxic waste management. It is one of the potential fields of application because geopolymer acts similar to zeolite materials, which have been known for their ability to absorb the toxic chemical wastes.

2.2. Corrosion of steel in concrete

The corrosion of the reinforcing steel is a major problem in concrete. Deterioration of concrete can be divided into three categories: chemical (or) physical deterioration of the concrete itself, physical damage, and corrosion of the reinforcement. Two main causes of corrosion of steel in concrete are carbonation and chloride attack [13]. Corrosion due to chloride attack will be studied in this paper. It is very important to know that chloride attack do not target the concrete, but the chloride ions makes their way to pass through the pores in the concrete to attack the steel.

The steel in concrete is usually in a non-corroding, passive condition. When chloride moves into the concrete, it damages the passive layer protecting the steel. The corrosion process involves the breaking down of the passive layer between the concrete and steel interface causing the steel to rust and pit. The chloride attack of steel reinforcement is shown in the figure 2.

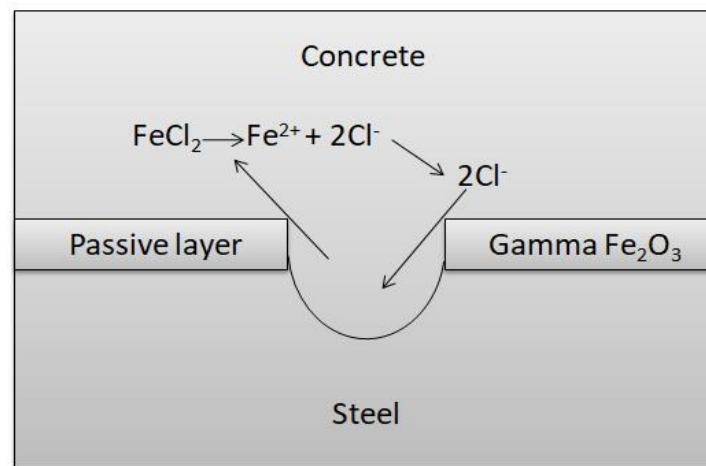


Figure 2 Chloride attack of steel reinforcement through concrete [14]

Once the passive layer starts to break down, corrosion begins to occur through anode and cathode reactions. When the steel in concrete starts to corrode, it dissolves into the pore water and gives up the electrons. These electrons will be consumed in the cathodic reaction which consumes water and oxygen to generate hydroxyl ions [14]. The anode and cathode reactions are only the first steps in the process of creating rust. This is followed by ferrous hydroxide becoming ferric hydroxide and then hydrated ferric oxide which is also known as rust.

The full corrosion process is explained in the figure 3.

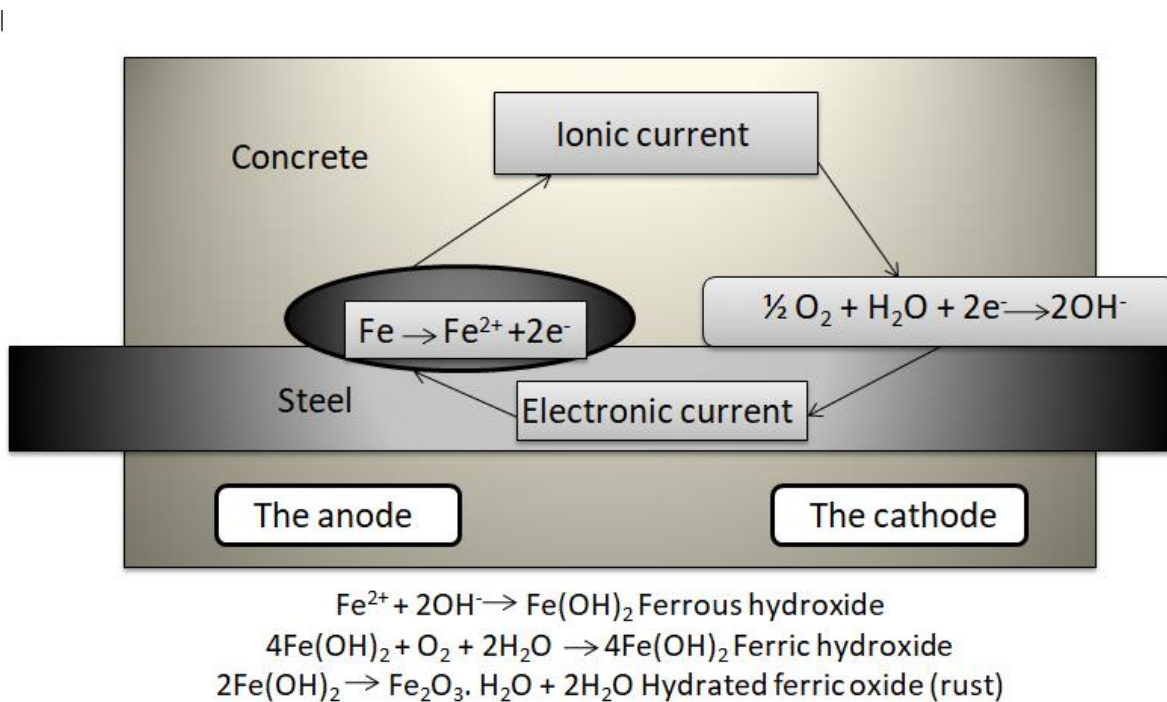


Figure 3 Corrosion reaction of steel reinforcement [14]

Unhydrated ferric oxide has a volume of about two times that of the steel it replaces when fully dense. When ferric oxide becomes hydrated, it starts swelling and becomes porous. This results in the increase of volume at the steel and concrete interface nearly 6 to 10 times of the original volume of the steel. This expansion of ferric oxide results in the cracking and spalling of concrete.

There are a variety of methods available for preventing the corrosion or at least to slow down the corrosion process. Galvanized reinforced steel can be used when the reinforcement will be exposed to the weather before construction begins. It can withstand chloride ion concentrations at least 4 to 5 times higher than the chloride level that causes in black steel reinforcement. Stainless steel reinforcement can be used, but is so expensive. Epoxy coatings can be used on rebar to give resistance to water, acids and alkali, but can affect the steel and concrete interface. It is also possible to slow down the corrosion process by following some aspects such as water content, concrete cover and compactness. Once the corrosion process starts, it is recommended to implement various repair methods to extend the service life of a structure. The cost of repairs can be minimized by delaying the corrosion and cracking process.

2.3. Corrosion of steel in GPC

Pawel et al [15] carried out experiments on Geopolymer ashes and coal derived products. The goal of the research was to study the corrosion resistance of Geopolymers to a number of chemical environments as well as the possibility of combining the new plastic with steel surfaces to prevent their corrosion. The experiment proved that Geopolymer is resistant to the action of acetone. The solutions of NAOH for each concentration of the solution were observed to move from the solution into the material, which resulted in the destruction of the material. Under high concentrations of HCL acid and the absence of a tight layer of the sediment the samples underwent rapid corrosion process. In other solutions, there was no case of corrosion and only the formation of the precipitate formed around the mineral compounds contained in the solution. They have concluded that the material has excellent corrosion resistance property which makes it possible to use such materials in industrial pipelines carrying concentrated acids.

Chandani et al [16] carried out long term tests on chloride ingress and steel corrosion in fly ash based geopolymer concrete. This study examined the initiation of chloride induced corrosion and the chloride permeability of geopolymer concrete in accelerated chloride environment using long term tests. The studies showed that chloride diffusion coefficient is less in fly ash and slag GPC than that of OPC concrete. With the increase of slag content in the binder, the diffusion coefficient decreased. When the slag content increases, the resultant binder consists of more calcium silicate hydrate, calcium aluminate silicate hydrate which have higher binding capacity for chloride ions to limit the ingress of those ions and higher amount of hydrotalcite phases which contains a layered double hydroxide structure that increases the capability to exchange ions with the concrete pore solutions and absorb anions to its structure. This results in the decreased diffusion coefficient. They have also concluded that the embedded rebar in fly ash and slag based GPC has higher resistance to corrosion than a rebar in OPC concrete.

Reddy et al [17] conducted an experiment on durability of reinforced GPC in the marine environment. This study evaluated the corrosion based durability of low calcium fly ash based GPC using beams that are centrally reinforced, made with 8M and 14M concentrations of NOAH and $\text{SiO}_2/\text{Na}_2\text{O}$ solutions. This experiment proved that GPC has better corrosion resistance performance compared to OPC. The test results indicated excellent resistance of the geopolymer concrete to chloride attack, with longer time to corrosion cracking, compared to OPC. This study also found that GPC is well bonded to the aggregates and is more homogeneous than OPC concrete.

Farhan et al [18] conducted an experimental study on the effect of corrosion on the bond between reinforcing steel bars and fibre reinforced geopolymer concrete. Three types of steel

fibres were used in this study including straight micro steel fibre, deformed steel fibre and hybrid steel fibre. This experiment proved that the addition of fibres improved the compressive strength and splitting tensile strength of geopolymer concrete mixes. The fibre reinforced geopolymer concrete improved the bond strength of reinforcing steel bar. This study also proved that the addition of steel fibres to the geopolymer concrete resulted in better resistance to chloride attack and corrosion than control plain geopolymer concrete specimens.

Babae et al [19] carried experimental study on chloride-induced corrosion of reinforcement in low-calcium fly ash-based geopolymer concrete. In this study, the performance of chloride-contaminated reinforced GPC specimens was investigated by parameters such as polarization resistance, open circuit corrosion potential and tafel slopes. The test results indicated that low-calcium fly ash based geopolymer concrete shows a comparable electrochemical performance to Portland cement concrete during the propagation stage of corrosion. The values of corrosion potential and polarization resistance after depassivation of the reinforcements were comparable to that of corrosion risk as expected for Portland cement based corroding systems. The polarization resistance values of geopolymer were comparable to Portland cement based corroding systems.

2.4. Half Cell Potential (HCP) method

A HCP is a non destructive technique used to find the corrosion risk of steels in reinforced concrete. It is very important to detect and evaluate the probability of corrosion for the maintenance of RC structure. By determining the status of corrosion in the early stage, a convenient repair solution can be planned for the damaged RC structures.

The cell potential (E_{cell}) is the measure of the potential difference between two half cells in an electrochemical cell. The potential difference is caused due to the ability of electrons to move from one half cell to the other. Electrons are able to move from one half cell to the other because the chemical reaction that takes place is a redox reaction. The cell potential (E_{cell}) is measured in terms of voltage V.

Wanchai et al [20] studied the influences of chloride content, concrete cover, moisture content and compressive strength on half-cell potential measurement and the relationship between the half-cell potential values and the corrosion level. This study was performed on concrete slabs with various dimensions. After curing of the specimens in water for 28 days, the half cell potential measurements were measured every week under wet and dry cycle for 140 days. This study proved that half-cell potential values decreased with the increase in chloride content and moisture content but increased with the increase in compressive strength.

According to ASTM C867 [21], the more negative values measured from the voltmeter, there is more probability of corrosion.

Table 2 Potential of cell vs probability of corrosion

cell potential (E_{cell})	Probability of corrosion
>-200 mV	10%
-200 to -350 mV	50%
< -350 mV	90%

2.5. Linear polarization resistance

Linear polarization resistance is an electrochemical technique used to measure the corrosion rates. It is the only corrosion monitoring method that allows corrosion rates to be measured directly in real time.

The corrosion rate can be computed by using the corrosion current (I_{CORR}) generated by the flow of electrons from anode to cathode. By applying the modified version of Faraday's law the following equation can be generated [22]:

$$I_{\text{CORR}} = 10^6 B/R_p \text{ } \mu\text{A}/\text{cm}^2 \quad (3)$$

Where R_p is the polarization resistance of a corroding electrode and is defined as the slope of a potential versus current density plot. The dimension of R_p is ohm-cm².

B is the Stern-Geary coefficient and the Stern-Geary coefficient is given by

$$B = b_a b_c / 2.303(b_a + b_c) \quad (4)$$

Where b_a and b_c are the anodic and cathodic Tafel slopes. B value is often taken as 25 mV for active corrosion state and 50 mV for passive conditions.

The corrosion rate in μm per year is given by

$$CR = 3.27 \times I_{\text{CORR}} \times E_w / \rho \quad (5)$$

Where

I_{CORR} is the corrosion current density in $\mu\text{A}/\text{cm}^2$

E_w is the equivalent weight of the corroding metal

ρ is the density of the corroding metal in g/cm^3

Gowers et al [23] performed linear polarization resistance mapping on site on two reinforced concrete structures. An alternative method has been studied by incorporating the monitoring bars of known area into concrete structure by physically defining the measurement area during LPR measurement to increase the accuracy of the results. They made a comparison between the LPR data and results obtained using potential plus resistivity mapping. This study concluded that a combination of potential and resistivity mapping is more effective in identifying the sites where the corrosion is active. This combination of results gave a good indication of the location and rate of corrosion of steel reinforced concrete structures. The advantage of this combination is the speed with which it can be carried out.

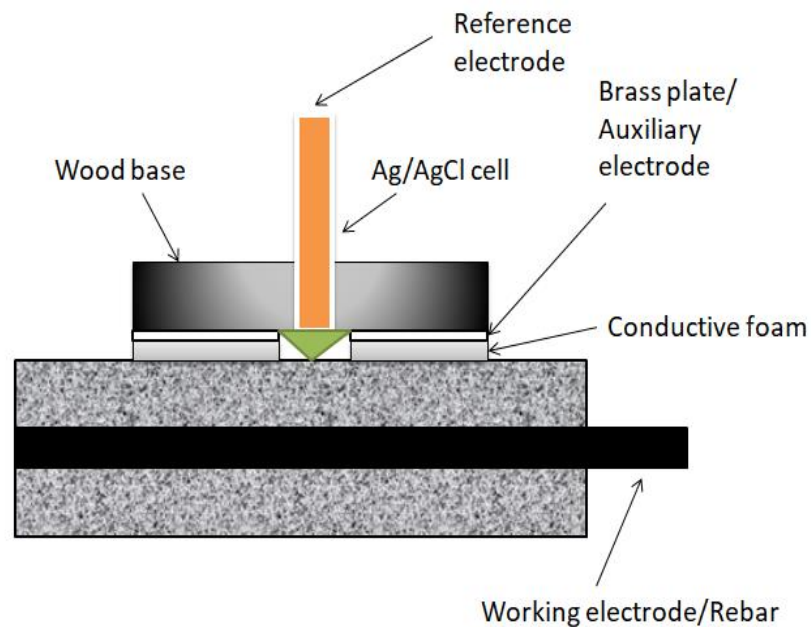


Figure 4 Linear Polarization Resistance Measurement Setup [23]

Model values of corrosion rates from LPR measurements are given in the following table:

Table 3 Typical corrosion rates from LPR measurement [24]

Corrosion rate	Corrosion rate i_{corr}	Corrosion penetration rate
Very low/negligible	$< 0.1 \mu\text{A}/\text{cm}^2$	$< 2 \mu\text{m}/\text{year}$
Low	$0.1\text{-}0.5 \mu\text{A}/\text{cm}^2$	$2\text{-}6 \mu\text{m}/\text{year}$
Moderate	$0.5\text{-}1.0 \mu\text{A}/\text{cm}^2$	$6\text{-}12 \mu\text{m}/\text{year}$
High	$>1.0 \mu\text{A}/\text{cm}^2$	$>12 \mu\text{m}/\text{year}$

Corrosion penetration rate is defined as the thickness loss of the material per unit of time due to the action of corrosion process. It is usually expressed in mils per year or millimetres per year or micrometers per year.

Andrade and Alonso [24] have explained in their study that for I_{CORR} values higher than $10 \mu\text{A}/\text{cm}^2$, the cross-section of the rebar decreases so drastically that it would result in a very rapid deterioration. For the I_{CORR} values ranging from $0.5\text{-}5 \mu\text{A}/\text{cm}^2$, the life time of the rebar varies between 20-50 years. On the other hand, I_{CORR} values less than $0.1 \mu\text{A}/\text{cm}^2$ have life times longer than 100 years.

The main objective of this project was to measure the durability of fly ash and bottom ash based Geopolymer concrete, compared to Ordinary Portland Cement, by means of accelerated corrosion testing of the reinforced rebar.

Chapter 3: Experimental setup

3.1. Materials

3.1.1. Precursor material

In the production of fly ash based geopolymer concretes, class F which is a low calcium fly ash is mostly used due to the low calcium content. For this project, a class F fly ash which was obtained from Centralia power plant Washington, USA. Based on ASTM C618 [25], three classes of fly ash (class N, F, C) are desired for use in GPC mix design but among those, class F were selected as it is a pozzolanic material and useful for developing the mix design.

The bottom ash used in this study was supplied by the Lafarge Power Plant Vancouver, Canada. This bottom ash was obtained from the pulverised coal combustion. The major components in bottom ash are silicon oxide, aluminium oxide and iron oxide. MgO, CaO, Na₂O and K₂O are also detected and are present in small quantities. The chemical composition of fly ash and bottom ash are showed in Table 4.

Table 4 Chemical Composition of fly ash and bottom ash

Compound	Fly ash (%)	Bottom ash (%)
SiO ₂	47.1	60.11
Al ₂ O ₃	17.4	14.35
Fe ₂ O ₃	5.7	5.92
CaO	14	10.40
MgO	5.4	4.49
SO ₃	0.8	0.10
Na ₂ O	N/A	2.232
K ₂ O	N/A	1.766
TiO ₂	N/A	0.892
P ₂ O ₅	N/A	0.200
Mn ₂ O ₃	N/A	0.093

3.1.2. Aggregates

The aggregates usually occupy about 70-80% of total volume. Fine aggregates and coarse aggregates used were obtained from a quarry in British Columbia with relative dry density (SSD)

of 2.671 and 2.713 respectively, and water absorption ratio of 0.79% and 0.69% respectively. The local aggregates comprising 12.5 mm used as coarse aggregates in GPC and the aggregates comprising 12.5mm and 6.5 mm used in OPC; the fine aggregates used in both OPC and GPC was medium coarse sand which was labelled for multipurpose use including concrete mixtures. These aggregates were kept in the oven for 24hrs and were prepared to be surface-saturated dry condition (SSD) before use.

3.1.3. Alkali activator

A combination of potassium silicate and potassium hydroxide was used as the alkaline activator.

Potassium hydroxide was obtained from Sigma-Aldrich, Canada with >85% purity in ACS grade. This was supplied in flakes form. The potassium hydroxide (KOH) solution was prepared by dissolving the flakes in water. The mass of KOH solids in a solution varies depending on the concentration of the solution expressed in terms of molar, M. The concentration of potassium hydroxide used was 12 Molar. The KOH solution was prepared 24 hours in advance of use by dissolving measured KOH pellets in required amount of tap water.

Potassium silicate powder (AgSil 16H) was obtained from PQ Cooperation (USA) was used in this project. Based on the MSDS file provided by the company, chemical composition of the K_2SiO_3 Powder was $K_2O = 32.4\%$, $SiO_2 = 52.8\%$ and water weight percentage of 14.8%.

Based on the literature review, it was suggested to prepare the K_2SiO_3 solution. However, several attempts were made to dissolve the K_2SiO_3 powder in hydroxide solution or tap water, were not successful. The solution turned into a gelatinous bulk at the bottom of the mixing bowl. To avoid this problem, K_2SiO_3 powder was first dry mixed with the fly ash, bottom ash and aggregates.

3.1.4. Ordinary Portland cement

ASTM Type 1 Portland cement was used for the manufacture of the control mix concrete. The controlled concrete mix was designed to achieve the strength and durability as per the structural requirements.

3.2. Preparation of Geopolymer and OPC concretes

The aggregates and bottom ash were prepared in saturated surface dry condition and kept in the plastic buckets with lid. The solid constituents of geopolymer concrete, i.e. the aggregates, fly ash and bottom ash were first mixed in dry condition in the pan mixer for about 2-3 minutes. Next, the potassium silicate powder was added to the mixture and mixed for a minute. The liquid part of the mixture, i.e. potassium hydroxide solution was added to the solids. Then the wet mixing is usually continued by adding the additional water required for another 5 minutes.

Table 5 Mix design of Geopolymer concrete

Material	Content (Kg/m ³)
Fly ash	194
Bottom ash	194
Coarse aggregates	1170
Sand	630
KOH (12M)	85.16
K ₂ SiO ₃	125.74

In order to prepare the OPC concretes, the dry ingredients such as cement, sand and coarse aggregates are mixed properly and the water is added slowly until the concrete is workable. Water plays a major role to make the concrete workable. Too much water can result in weak concrete and too little water can result in unworkable concrete. The mix design for the 40 MPa concrete is shown in the table 6.

Table 6 Mix design of OPC concrete

Material	Kg/m ³
Cement	400
Sand	660
12.5 mm aggregate	701
6.5 mm aggregate	467
Water	160

3.3. Specimen preparation

In this project two different types of samples were used: 6"x 6"x 21" beam samples and 4"x 8" cylindrical samples. The beam specimens were used in the corrosion study and the cylindrical samples were used in determining the compressive strength of the geopolymer concrete mix and OPC mix.

Plywood of $\frac{3}{4}$ " thickness is used in construction of beam molds of 6"x6"x21" dimensions of height, width and length respectively as shown in the figure 10. The same mix design is used for both cylinders and beams.

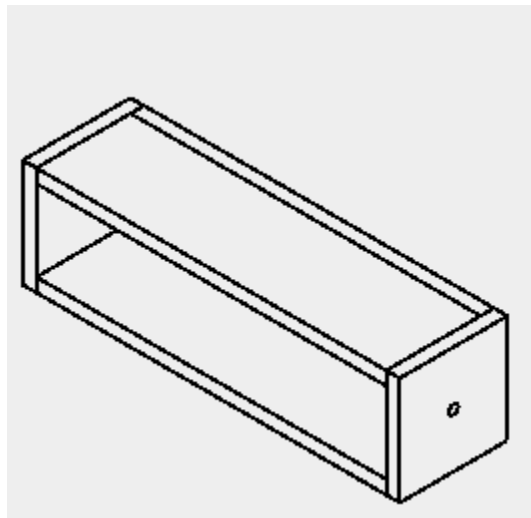


Figure 5 Model diagram of beam mold

3.4. Curing temperature and conditions

The geopolymer concrete test specimens were allowed to set in the molds for one day at room temperature before being demolded. After demolding, the specimens were kept in the oven at 80°C for 24 hours. After that, the specimens were cured in room temperature in water tank until they reached the 28th day of age. Heat curing is recommended for low calcium based geopolymer concrete. Heat curing promotes the chemical reaction that occurs in the

geopolymer concrete. It can be achieved by either dry-curing or steam-curing. Curing time and curing temperature influence the compressive strength of geopolymer concrete.

After the 28th day, the cylinders were taken out from the water tank and the surfaces are grounded using a grinding machine. This ensures the distribution of load uniformly for a compression test. These specimens were rested in the ambient condition until SSD condition was achieved.

3.5. Compressive strength test

Compression test of the cylinders was conducted using Forney's compressive test machine in the materials lab by following ASTM C39-14[26].

Before starting the test, calculate the diameter and area of each concrete specimen. Then the cylinder was placed in the center of the loading area. The cylinder must be placed on top of the neoprene cap and set the loading rate to about 0.3 MPa/s. The loading rate was remained constant until the concrete cylinder starts to fail. The concrete test is complete when the cylinder begins to crack and splinter. Stop the test, open the cage door and safely remove the cracked concrete. The recorded maximum load value is in kN and it can be converted into the compressive strength in MPa by dividing the cross-sectional area of the cylinder.



Figure 6 Forney's Compressive Strength Test Machine

3.6. Experimental program

3.6.1. Test specimens

For the experimental program, 6"X6"X21" beam specimens, centrally reinforced with ½" steel rebar were prepared. One end of the rebar was extended so electrical connections could be made. After curing for 24 hours at 80°C, the samples were kept in the water tank.

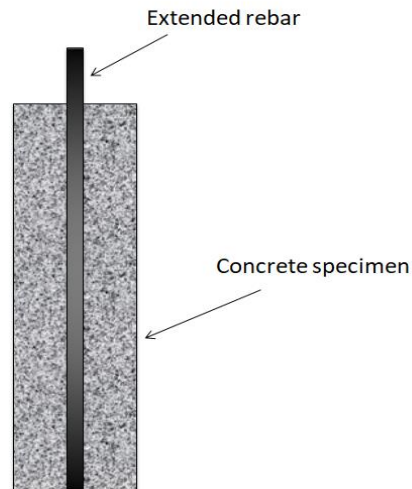


Figure 7 Schematic diagram of beam specimen

3.6.2. Testing apparatus and materials

A Rubbermaid tank with chloride solution was used for holding the beam specimens. A 12 gauge Copper wire was used to connect the rebar and the stainless steel rod to the power supply. A 30V D.C. power supply was used to provide the electric potential to the rebar. A digital multimeter was used to ensure the voltage across the circuit was constant and also for reading the current passing through the beams. A 3.5% chloride solution was prepared in the Rubbermaid tank as this can be comparable to the typical salt concentration in sea water. This concentration will show better performance of the rebar. An epoxy coating was applied to the exposed rebar to avoid crevice corrosion.

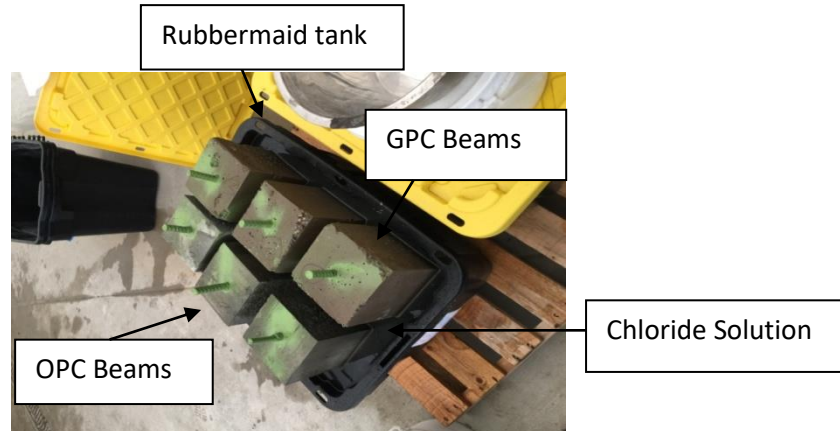


Figure 8 Beam specimens immersed in a chloride solution

3.6.3. Chloride solution

A commercially available product called 'Instant Ocean' was used to prepare the chloride solution. According to ASTM D1141 [27] for artificial seawater, the 'Instant Ocean' product was able to generate a chloride solution that is similar to natural seawater.

In order to prepare 3.5% NaCl solution, 17.50 kgs of NaCl was added to every 50 litres of water and stirred with a mixing rod properly until the product completely dissolves into the water.

3.7. Accelerated reinforced corrosion

An accelerated electro-chemical laboratory method, first developed by the Nordest method [28], followed by the Florida Department of Transportation [29] was used in this experiment. This method was used to test corrosion resistance of various concrete mixes using centrally reinforced concrete samples in a chloride solution. A constant voltage is applied to all the samples and the current to each specimen is measured. The specimen starts to show signs of corrosion when there is a rise in the current.

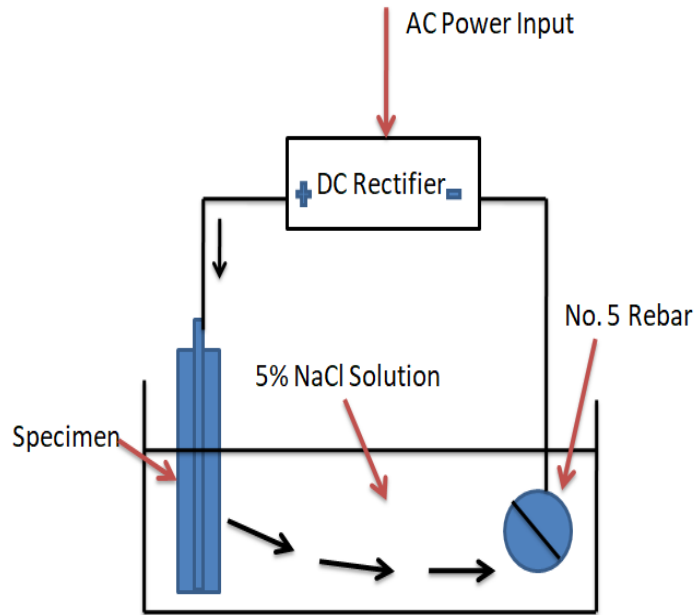


Figure 9 FDOT Accelerated corrosion test setup [29]

In this experiment, the durability of fly ash based geopolymer concrete was tested using an accelerated corrosion method. Corrosion resistance of GPC was tested against OPC in a chloride solution.

3.8. Test procedure

The Rubbermaid tank was filled with the chloride solution that would allow each beam to be partially immersed. After 28 days of curing in the water at ambient temperature, the beams were placed in a chloride solution for a period of 28 days. This helps to keep the initial D.C. power to a manageable low value. After that, the extended side of rebar acting as an anode was connected to a 30V power supply. This high voltage accelerates the corrosion process and decreases the test period time. A Stainless steel rod was used to act as a cathode. The D.C. power supply was turned on and set to 30V electrical potential.

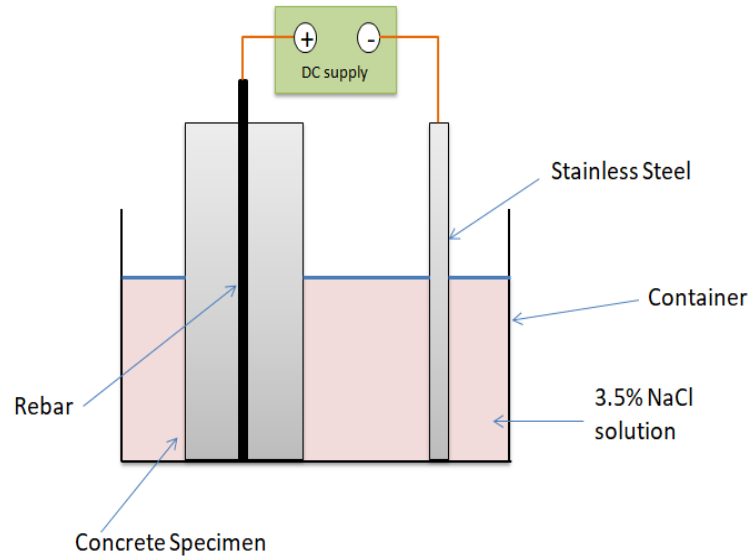


Figure 10 Schematic of Accelerated Corrosion test setup

Once the testing procedure started, current readings were taken every day. A rise in the current indicated the beginning of corrosion process, and eventually the start of the formation of cracks in the beams. Once the beams reached the high current, there were visible signs of corrosion in the chloride water and cracking of beams and the beams were considered to be failed. The time taken to initiate the corrosion in the rebar in geopolymer concrete is higher than that of OPC concrete. The beams were removed from the chloride water and left to air dry for 24 hours. After that, the beams were tested for rate of corrosion using LPR. The final step involved breaking the OPC and GPC beams to determine the effects of corrosion on rebar by measuring the mass loss of the steel rebar for each beam.

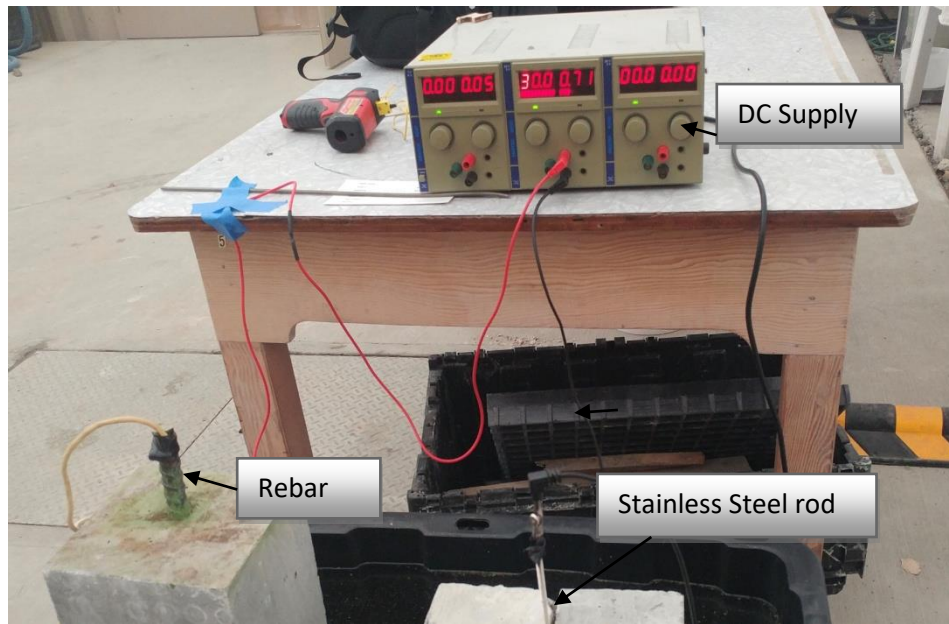


Figure 11 Experimental setup for Accelerated Corrosion test

3.9. Half cell potential

Half cell potential (HCP) is an effective method that has been used by many researches across the world. It is a method of assessing invisible corrosion of reinforced concrete without destructing the samples. HCP provides information about probability of corrosion.

A digital voltmeter is used to read the potential difference values between the external reference electrode and reinforced steel rebar. The positive terminal of the voltmeter is connected to the reinforced steel rebar in a concrete beam. The negative terminal of the voltmeter is connected to the half cell electrode/Reference electrode. The copper/copper sulphate was used for reference electrode. If the surface of the concrete is too dry, pre-wetting is required. A pre wetted sponge is used to ensure proper surface contact between the concrete surface and the tip of half cell electrode.

For a consistent reading, a center line with a pre defined equal spacing of three measuring points at 7 inches distance was marked on the surface of the concrete. The potential values for these three points were recorded from the voltmeter for both OPC and GPC beams.

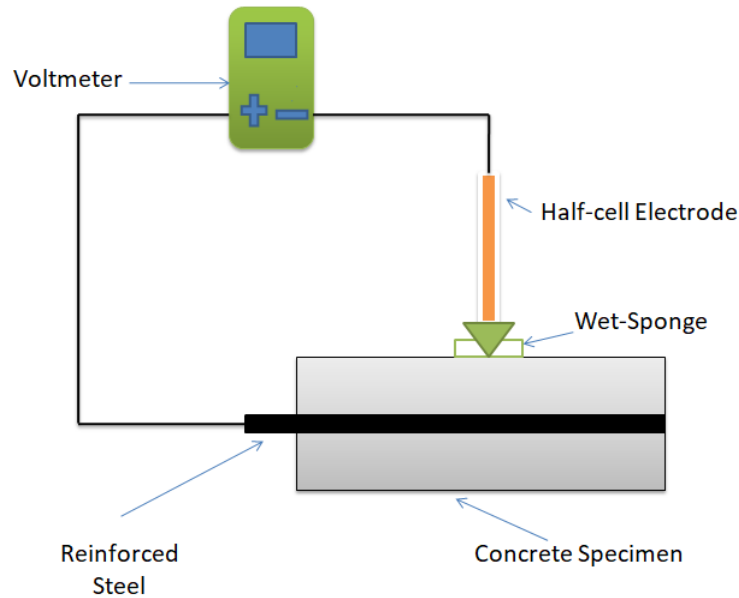


Figure 12 Schematic of the Half-cell potential measurement setup

3.10. Linear Polarization Resistance Test

The linear polarization resistance method is a non destructive testing method used to measure the corrosion rate. The data graph obtained from the instrument can be used to calculate the corrosion rate. Polarization resistance measurements are an accurate and rapid technique to measure the rate of corrosion.

After the specimens were removed from the chloride water and left to air dry for 24 hours, the LPR test was performed. The specimens were supported on a wooden surface, which helps the specimen to be on a flat surface. To conduct the LPR test, Gamry Instruments Reference 600+ potentiostat was used. The cell cable was connected to reference electrode, counter electrode, rebar and ground. If the surface of the concrete is too dry, pre-wetting is required. A pre wetted sponge is used to ensure proper surface contact between the concrete surface and the tip of reference electrode. The equipment is connected to a computer to read the data graph. A complete setup of the Gamry Potentiostat is shown in the figure 13. The Gamry Echem Analyst Software was used to run the experiment. This is a single program that runs data-analysis for all type of experiments such as DC Corrosions, EIS and Physical Electrochemistry. Before running the software, the experimental Setup values are entered manually.

For a consistent reading, a center line with a pre defined equal spacing of three measuring points at 7 inches distance was marked on the surface of the concrete. The LPR data graphs for these three points were recorded in the computer for both OPC and GPC beams.

The following values have been used in the LPR measurement:

$$E_w = 27.92$$

$$\rho = 7.85 \text{ g/cm}^2$$

B = 25 mV as the steel rebars inside the concrete showed 90% probability of corrosion.

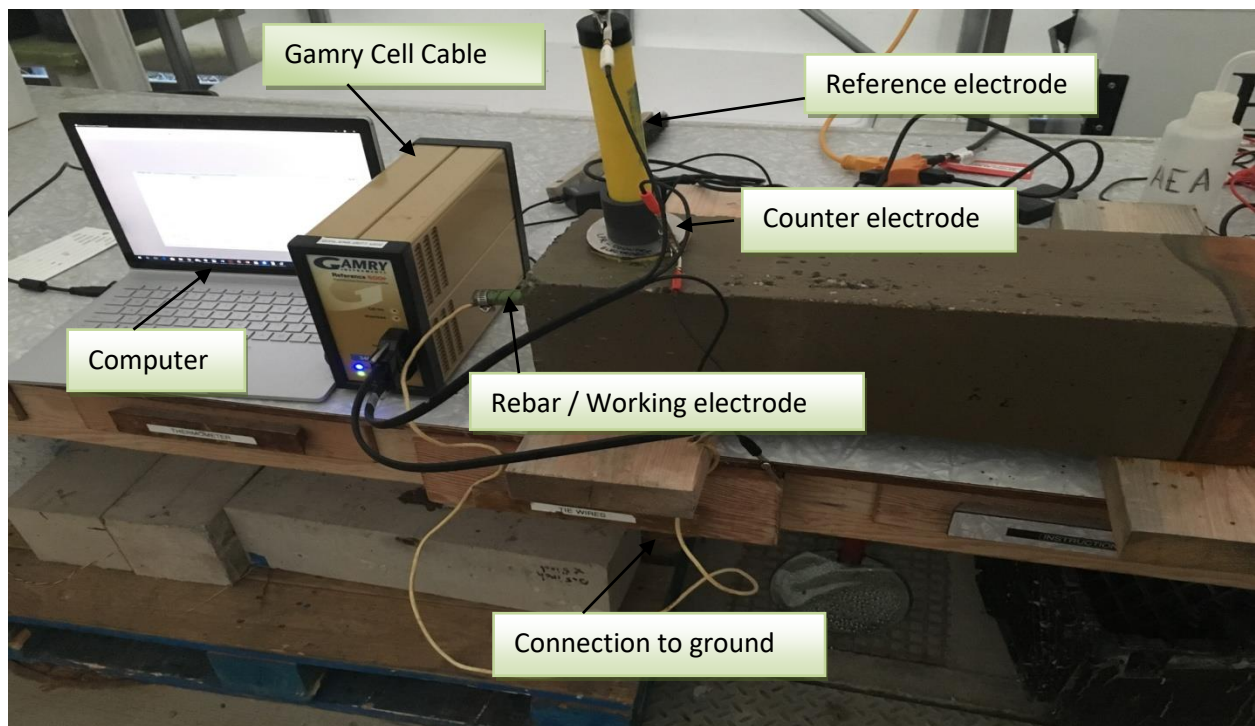


Figure 13 Gamry Potentiostat setup for LPR test

3.11. Residual Flexural Load Test

Corrosion in steel reinforcement is one of the reasons for early degradation of the concrete structure. Due to the accelerated corrosion process, there is a formation of corrosion in the steel reinforcement and formation of cracks in the concrete structure. This results in mass loss and reduces the stiffness of the specimen. After the accelerated corrosion process, recording

half-cell potential and linear polarization resistance tests, flexural load test was performed on the beams to determine the loading capacity of the beams. MTI- 50K universal testing machine is used with center point loading method. Figure 18 shows MTI-50K loading machine performing the flexure loading test on the specimens.

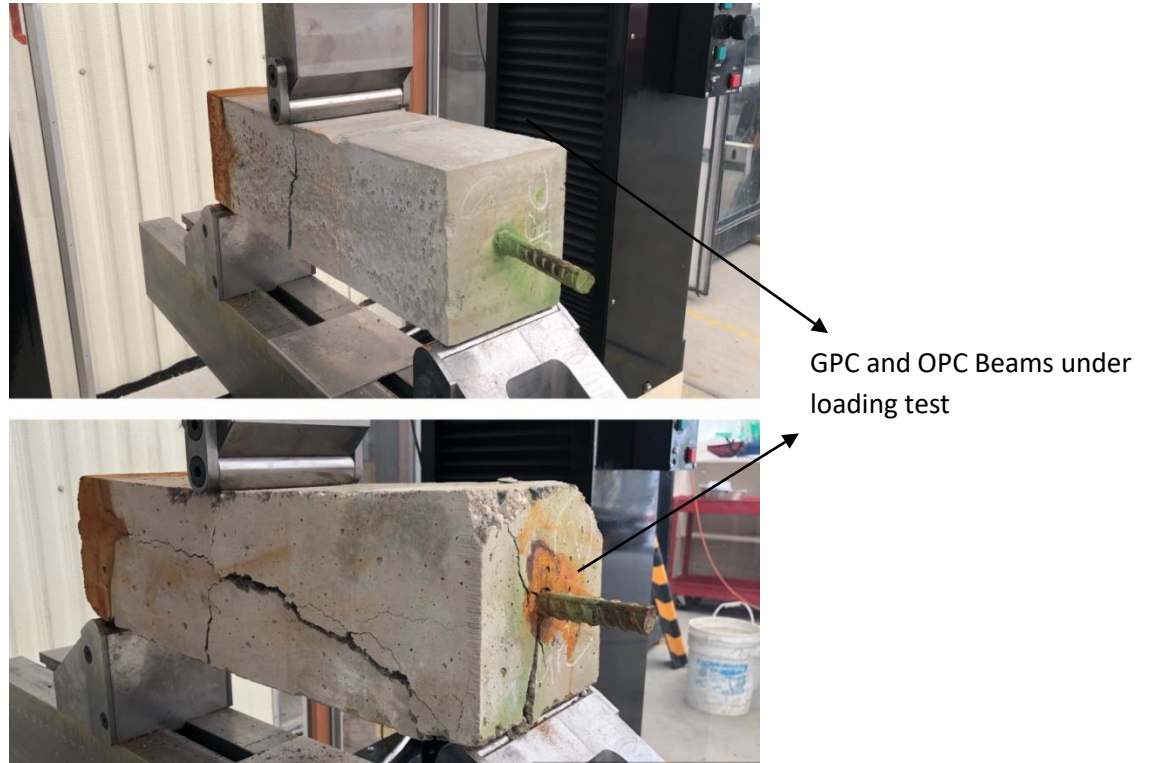


Figure 14 Specimens under center point loading test

Chapter 4: Experimental results and discussion

4.1. Compressive strength

The compressive strength of the different types of OPC and GPC concretes was measured for 4"X8" cylinders. The cylinders were tested at 7 days and 28 days of age after casting and steam curing in the oven at 80°C for 24 hours in case of geopolymer cylinders and cured in ambient temperature for OPC cylinders. A minimum of three GPC and three OPC cylinders were used in this test. The average compressive strength of the GPC cylinders at 7 days and 28 days were 26.65 MPa and 31.70 MPa respectively. For the OPC, the strengths were 26.93 MPa and 33.67 MPa respectively. It can be concluded from the results that both GPC and OPC cylinders cured after 28 days are stronger than those were only cured for 7 days.

Table 7 Compressive strength development of OPC and GPC beams

S.No	Specimen (cylinders)	Compressive strength after 7 days (MPa)	Compressive strength after 28 days (MPa)
1	GPC 1	25.95	32.02
2	GPC 2	26.34	30.82
3	GPC 3	27.67	32.27
4	OPC 1	25.56	33.28
5	OPC 2	26.78	33.65
6	OPC 3	28.46	34.08

4.2. Cracking behaviour of the beams

The OPC beams started to show signs of rusting after 60 hours of accelerated corrosion testing. On the other hand, the GPC beams showed no signs of rust for the same period of time. The brown rust stain seen on top of the OPC beams is the first visual evidence of corrosion in the embedded steel. It was also observed that corrosion products were floating on the surface of chloride solution. After nearly 200 hours, a crack was observed in the OPC beams. On the other hand, there were no cracks observed in the GPC beams. This makes it clear that GPC beams are highly durable than OPC beams. The accelerated corrosion test was stopped at 300 hours and the beams were removed from the chloride solution tank. Further the beams were visually inspected and tested for corrosion potential and corrosion rate using HCP and LPR.



Figure 15 OPC beam after 200 hours of test



Figure 16 GPC beam after 200 hours of test

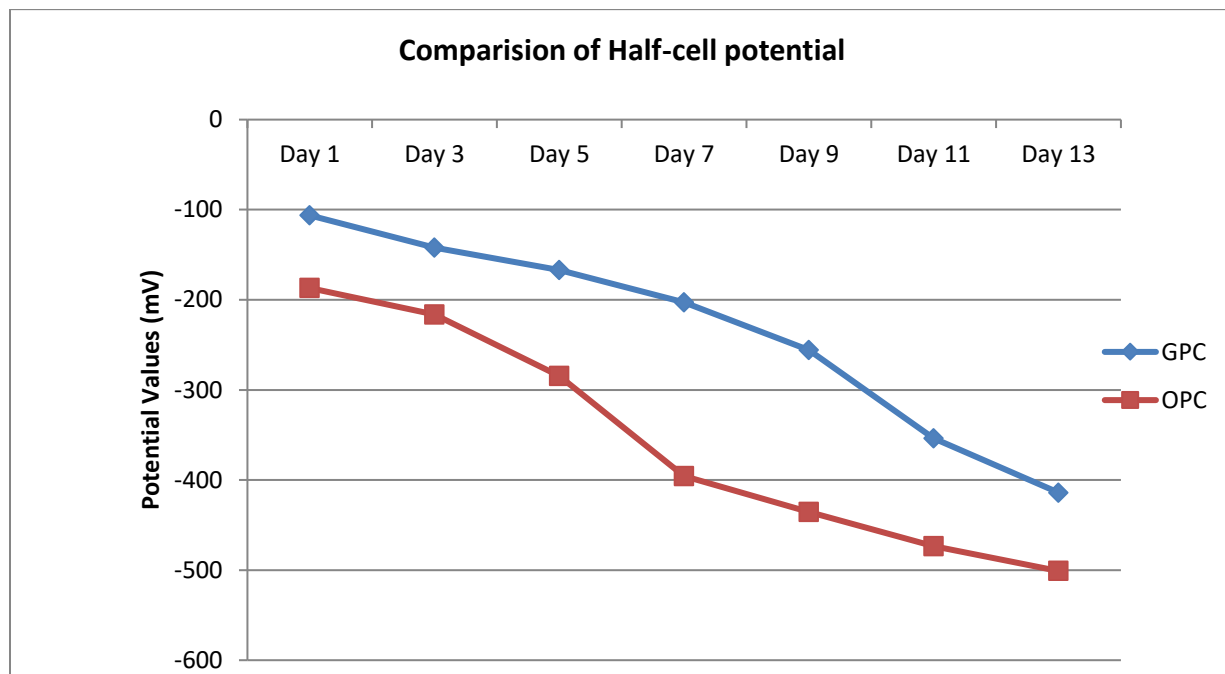
4.3. HCP analysis

Before performing the accelerated corrosion test, the initial half cell potential readings on day 1 were taken from the voltmeter for both OPC and GPC beams. There was three measuring points on each specimen and the potential values for these three points were recorded and their total was averaged. These readings were taken on alternative days until the test reached 300 hours.

Table 8 represents the half cell potential values of GPC and OPC specimens.

Table 8 Half cell potential test results

Specimen	Half cell potential (mV)						
	Day 1	Day 3	Day 5	Day 7	Day 9	Day 11	Day 13
GPC 1	-93	-127	-147	-165	-220	-310	-370
GPC 2	-101	-132	-160	-217	-268	-362	-425
GPC 3	-125	-167	-196	-228	-279	-389	-447
OPC 1	-190	-220	-287	-390	-439	-467	-490
OPC 2	-173	-200	-269	-387	-420	-455	-489
OPC 3	-198	-229	-298	-410	-447	-498	-524

**Figure 17 Average HCP values of OPC and GPC Beams**

It can be observed that the half-cell potential values are more negative from day 1 to day 13 for both the specimens as shown in figure 17. On day 1 the initial potential value of GPC beam 1 was recorded as -93 mV, whereas the potential value of OPC beam 1 was recorded as -190 mV. The trend line of both GPC and OPC specimens is in a decline manner, which indicates an increase in the probability of corrosion from day 1 to day 13. After day 13, both the specimens showed 90% of probability of corrosion.

4.4. LPR analysis

The LPR technique is used for accurately measuring the corrosion rates of the specimens and the results are tabulated in table 9. The corrosion rate is calculated by using the equations discussed in literature review in section 2.5. This data gives more detailed information on the structural condition. The experiments are conducted for Geopolymer concrete specimens and cement concrete specimens using Gamry Potentiostat. The graphical data for all the specimens are shown in the below figures:

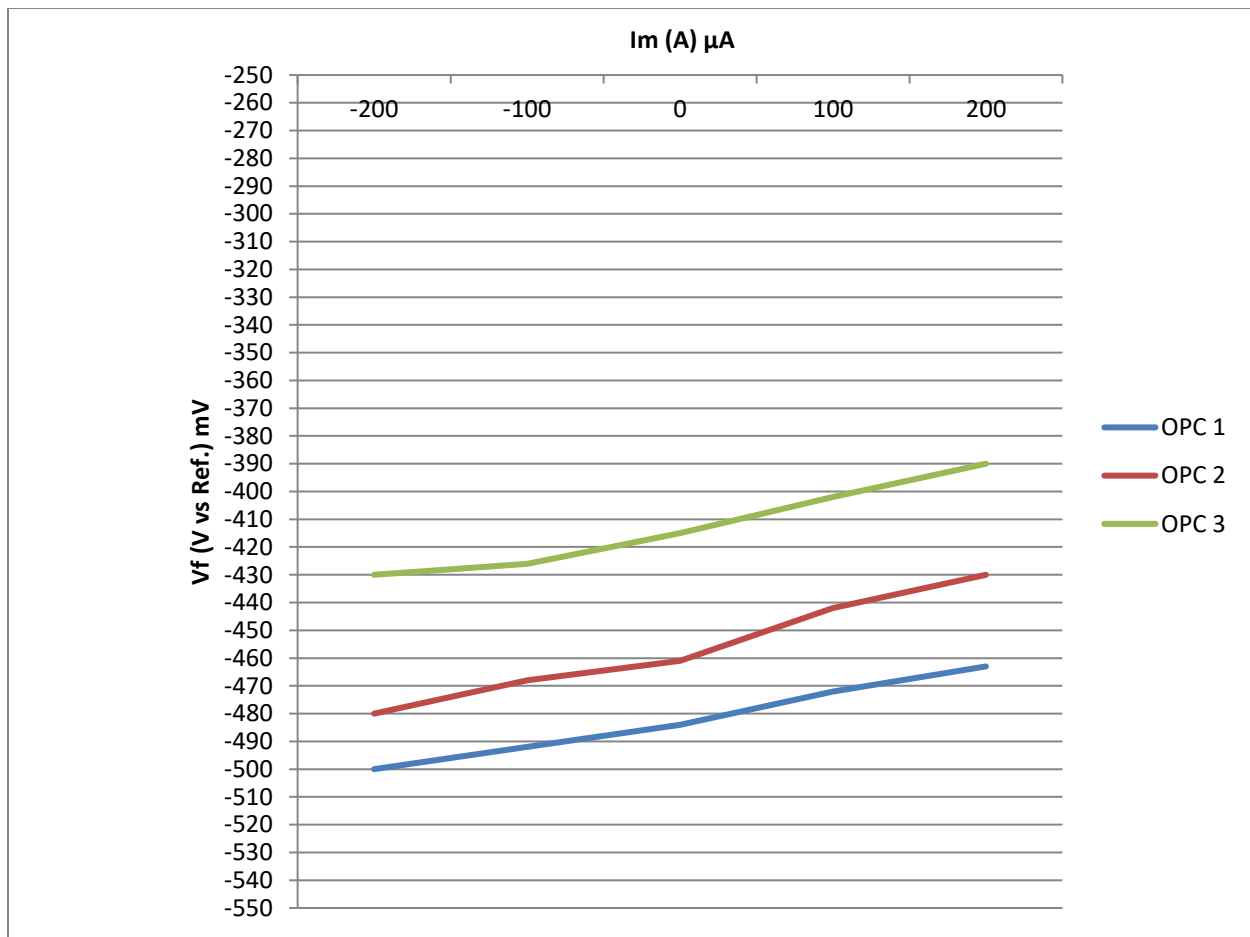


Figure 18 LPR graphical data of OPC beams

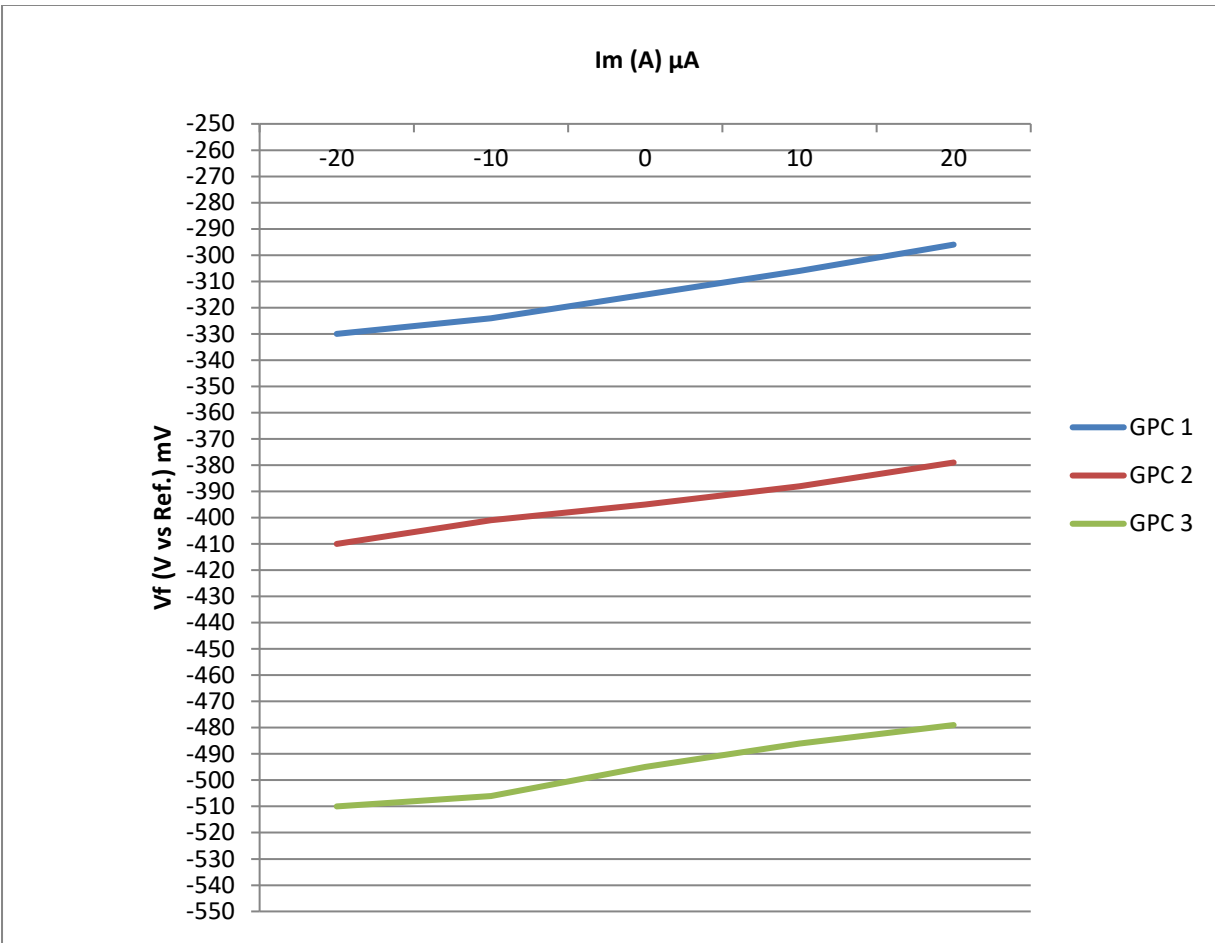


Figure 19 LPR graphical data of GPC beams

Table 9 Linear polarization resistance test results

S.NO.	Type of Specimen	Corrosion Current I_{CORR} ($\mu A/cm^2$)	Corrosion rate ($\mu m/year$)	Corrosion condition (ASTM standard)
1.	GPC 1	0.9113	10.598	Moderate
2.	GPC 2	1.2303	14.308	High
3.	GPC 3	1.7429	20.270	High
4.	OPC 1	4.9214	57.233	Very high
5.	OPC 2	4.1010	47.696	Very high
6.	OPC 3	5.0471	58.698	Very high

The corrosion rate of the geopolymer concrete specimens is in between 10 $\mu\text{m}/\text{year}$ and 20 $\mu\text{m}/\text{year}$. This indicates that these specimens have moderate to high rate of corrosion. No cracks were observed on the surface of the GPC specimen, but micro cracks may have occurred in the surrounding areas of the bar due to the corrosion products that was build up inside, which might have allowed some chloride ions to penetrate into the bar. Whereas, the corrosion rate of the OPC specimens is in between 40 $\mu\text{m}/\text{year}$ and 60 $\mu\text{m}/\text{year}$, which indicates very high rate of corrosion.

From the results it can be seen that GPC 1 had the best corrosion resistance. It gave the lowest corrosion rate. We can see the geopolymer concrete shows better results for corrosion rate compared to ordinary Portland concrete, is a proof of their compactness, and the subsequent resistance to chloride penetration. The permeability and electric resistivity of the GPC concrete was not affected by the severe chloride environment in the perspective of reduced cracking. Hence the geopolymer concrete can be utilized in marine environment.

4.5. Residual Flexural Load

After the HCP and LPR testing, the beams were tested for residual load with center-point loading to find out the loading capacity using universal MTI-K testing machine. The results of the flexural tests are shown in Table 10.

Table 10 Residual Flexural Loads of all the beams

Specimen Type	Flexural Load (N)
GPC 1	19678
GPC 2	20678
GPC 3	19325
OPC 1	14789
OPC 2	15908
OPC 3	16342

The table represents that the loading capacity of the OPC beams is less as compared to the GPC beams. The average flexural strength for the OPC was 4.5 MPa and for the GPC was 6 MPa. This test was carried after nearly 90 days of casting the beam specimens.

4.6. Mass loss measurements

The corrosion assessment of steel bars used in the reinforced concrete can be done by mass loss measurements. The initial mass of each rebar are recorded before the casting procedure. After HCP and LPR experiments, the beams were completely broken to restore the entire rebar.



Figure 20 Broken OPC and GPC Beams

The rebars were cleaned with deionised water and a metal brush was used to remove the corrosion products from the rebars. The steel rebars showed critical corrosion damage for the OPC beams, while the rebars from the GPC beams showed less damage compared to OPC beams. The more negative values observed in GPC beams however, is not a necessary indication of high risk of corrosion. This can happen due to a number of reasons such as lack of oxygen at the steel and concrete interface due to oxygen depletion, binding of the chloride ions or lower pH level in geopolymer binders compared to OPC binders [30]. After that, these rebars

were weighed and recorded as final mass. Then the percentage of mass loss is calculated for both OPC and GPC beams.

Table 11 Percentage of mass loss of reinforced rebar

Specimen Type	Initial mass (gms)	Final mass (gms)	Mass loss (%)
GPC 1	944.5	914.9	3.13
GPC 2	945.5	906.4	4.13
GPC 3	941.9	894.5	5.16
OPC 1	941.9	756.8	21.80
OPC 2	944.3	786.3	16.73
OPC 3	943.7	759.4	19.52

The percentage mass loss for the GPC beams were 3.13%, 4.13% and 5.16% respectively, whereas, for the OPC beams it is 21.80%, 16.73% and 19.52% respectively. The OPC beams showed huge mass loss due to the crack formation which makes the chloride ions to penetrate quickly into the concrete and increase the rate of corrosion.

Chapter 5: Conclusions

The primary aim of this project was to experimentally study the corrosion resistance of bottom ash and fly ash based reinforced geopolymer concrete, compared to Ordinary Portland Cement concrete. By analyzing the test results, the following conclusions can be drawn.

- ❖ The average compressive strength of fly ash based geopolymer concrete is similar to OPC concrete which makes it suitable for structural applications. The average strengths of GPC cylinders at 7 days and 28 days were 26.65 MPa and 31.70 MPa respectively. For the OPC, the strengths were 26.93 MPa and 33.67 MPa respectively. It can be concluded from the results that both GPC and OPC cylinders cured after 28 days are stronger than those were only cured for 7 days.
- ❖ After nearly 200 hours of accelerated corrosion test, a crack was observed in the OPC beams. On the other hand, there were no cracks observed in the GPC beams. This makes it clear that GPC beams are highly durable than OPC beams.
- ❖ The Half-Cell Potential values decreased for both the specimens during the test period. The trend line of both GPC and OPC specimens is in a decline manner, which indicates an increase in the probability of corrosion from Day 1 to Day 13. After day 13, both the specimens showed 90% probability of corrosion.
- ❖ The corrosion rate of the geopolymer concrete specimens is in between 10 $\mu\text{m}/\text{year}$ and 20 $\mu\text{m}/\text{year}$. This indicates that these specimens have moderate to high rate of corrosion. Whereas, the corrosion rate of the OPC specimens is 40 $\mu\text{m}/\text{year}$ and 60 $\mu\text{m}/\text{year}$, which indicates very high rate of corrosion. This proves the geopolymer concrete possesses better results for corrosion rate compared to ordinary Portland concrete and hence the geopolymer concrete can be utilized in marine environment.
- ❖ The loading capacity of the OPC beams is less as compared to the GPC beams.
- ❖ The percentage mass loss for the GPC beams were 3.13%, 4.13% and 5.16% respectively, whereas, for the OPC beams it is 21.80%, 16.73% and 19.52% respectively. The OPC beams showed huge mass loss due to the crack formation which makes the chloride ions to penetrate quickly into the concrete and increase the rate of corrosion.
- ❖ The studies have shown that the performance of geopolymer concrete specimens is comparable to that of OPC concrete with respects to reinforced corrosion.

This research has shown a few properties of geopolymer materials to enable its use as a building material. The geopolymer materials possess a higher resistance to the corrosive activity of salt solutions compared to OPC. This makes a possibility to use geopolymer in industrial pipelines and marine environments. All the results look very promising, but require broader study to make sure the correctness of the results.

References

- 1) "Steel in the sound concrete." [online]. Available: https://www.concretecorrosion.net/html_en/mecanism/contenu.htm [Accessed: 17-August-2017].
- 2) J. Davidovits , "Properties of Geopolymer Cements and Concretes," Scientific Research Institute on Binders and Materials, Kiev State Technical university, Ukraine, pp. 131-149 1994.
- 3) H. Xu and J. S. J. Van Deventer, "The geopolymerization of alumino-silicate minerals," International Journal of Mineral Processing, vol. 59, no. 3, pp. 247-266, Jun. 2000.
- 4) P. Duxson, A. Fernandez-Jimenez , and others, "Geopolymer Technology: the current state of the art," J Mater Sci, pp. 2917-2933, 2007.
- 5) "Coal Ash, Fly Ash, Bottom Ash, and Boiler Slag." [online]. Available: <https://www.nrdc.org/onearth/coal-ash-fly-ash-bottom-ash-and-boiler-slag> [Accessed: 20-January-2018].
- 6) S. V. A. Silva, C. L. Wijewardena, S. M. A. Nanayakkara, and others, "Development of fly ash based geopolymer concrete," 2012.
- 7) S. E. Wallah and B. V. Rangan, "LOW-CALCIUM FLY ASH-BASED GEOPOLYMER CONCRETE: LONG-TERM PROPERTIES," Research report GC2, Faculty of Engineering, Curtin University of Technology , Perth, Australia, 2006.
- 8) M. Mustafa Al Bakri, S. N. Fifinatasha and others, "Reviews on the Different Sources Materials to the Geopolymer Performance," Advances in Environmental Biology, vol. 12. No. 7, pp. 3835-3842, Oct. 2013.
- 9) H. Tchakoute Kouamo, J. A. Mbey, and others, "Synthesis of volcano ash-based geopolymer mortars by fusion method: Effects of adding metakaolin to fused volcanic ash," Ceramics International, Vol. 39, pp. 1613-1621, 2013.
- 10) J. Davidovits, "Geopolymer Chemistry & Applications," 4th edition, Nov. 2015.
- 11) J. Davivits, "Geopolymer Chemistry and Properties," paper presented at the Geopolymer '88, First European Conference on Soft Mineralurgy," Compiegne, France, 1988.
- 12) J. Davidovits, "30 years of Successes and Failures in Geopolymer Applications. Market Trends and Potential Breakthroughs," Geopolymer Conference, Melbourne, Australia, 2002.
- 13) V. Primoz, "Corrosion in concrete steel," University of Ljubljana, Faculty of mathematics and physics, Department of physics, Kamnik, Apr. 2008.
- 14) John P. Broomfield, "corrosion of steel in concrete," understanding, investigation and repair, 2nd edition, London, UK.

- 15) M. Pawel, M. Janusz, and S. K. Jerzy, "THE CORROSION RESISTANCE OF THE BASE GEOPOLYMER FLY ASH," *Advances in Science and Technology Research Journal*, Vol. 7, No. 19, pp. 88-92, Sept. 2013.
- 16) T. Chandani, S. Ahmad, and others, "Chloride ingress and steel corrosion in geopolymer concrete based on long term tests," *Materials and Design*, Vol. 116, pp. 287-299, 2017.
- 17) D. V. Reddy, and others, "DURABILITY OF REINFORCED FLY ASH-BASED GEOPOLYMER CONCRETE IN THE MARINE ENVIRONMENT," 36th Conference on Our World in Concrete & Structures, Singapore, Aug. 2011.
- 18) Nabeel A. Farhan, M. Neaz Sheikh, Muhammad N.S. Hadi, "Experimental Investigation on the Effect of Corrosion on the Bond Between Reinforcing Steel Bars and Fibre Reinforced Geopolymer Concrete." *Structures*, Vol. 14, pp. 251-261, 2018.
- 19) M. Babae, A. Castel, "Chloride-induced corrosion of reinforcement in low-calcium fly ash-based geopolymer concrete," *Cement and Concrete Research*, Vol. 88, pp. 96-107, 2016.
- 20) Y. Wanchai, P. Thanawit, "Factors influencing half-cell potential measurement and its relationship with corrosion level," *Measurement*, Vol. 104, pp. 159-168, 2017.
- 21) "Standard Test Method for Corrosion Potentials of Uncoated Reinforcing Steel in Concrete," *ASTM International Standards: C876-15*, 2015.
- 22) "Standard Test method for Conducting Potentiodynamic Polarization Resistance measurements," *ASTM International Standards: G59-97*, 2002.
- 23) K. R. Gowers and S. G. Millard, "ON-SITE LINEAR POLARIZATION RESISTANCE MAPPING OF REINFORCED CONCRETE STRUCTURES," *Corrosion Science*, Vol. 35, Nos. 5-8, pp. 1593-1600, 1993.
- 24) C. Andrade, C. Alonso, "Corrosion rate monitoring in the laboratory and on site," *Construction and Building Materials*, Vol. 10, No. 5, pp. 315-328, 1996.
- 25) "Standard Specification for Coal Fly Ash and Raw or Calcined Natural Pozzolan for Use in Concrete," *ASTM International Standards: C618-12a*, 2014.
- 26) "Standard Test Method for compressive strength of Cylindrical concrete Specimens," *ASTM International Standards" C39/C39M- 14*, 2014.
- 27) "Standard Practice for the Preparation of Substitute Ocean Water," *ASTM International: D 1141-98*, 2003.
- 28) Nordtest, "Nordtest Method," Espoo, Finland, 1989.
- 29) Florida Department of Transportation, "Florida Method of Test for an Accelerated Laboratory Method for Corrosion Testing of Reinforced Concrete Using Impressed Current," FM 5-522, FDOT, 2000.
- 30) C. Gunasekar, S. Bhuiyan, and others, "Corrosion resistance in different fly ash based geopolymer concretes," 2017.

Appendix A: LPR data graph of the OPC and GPC beams

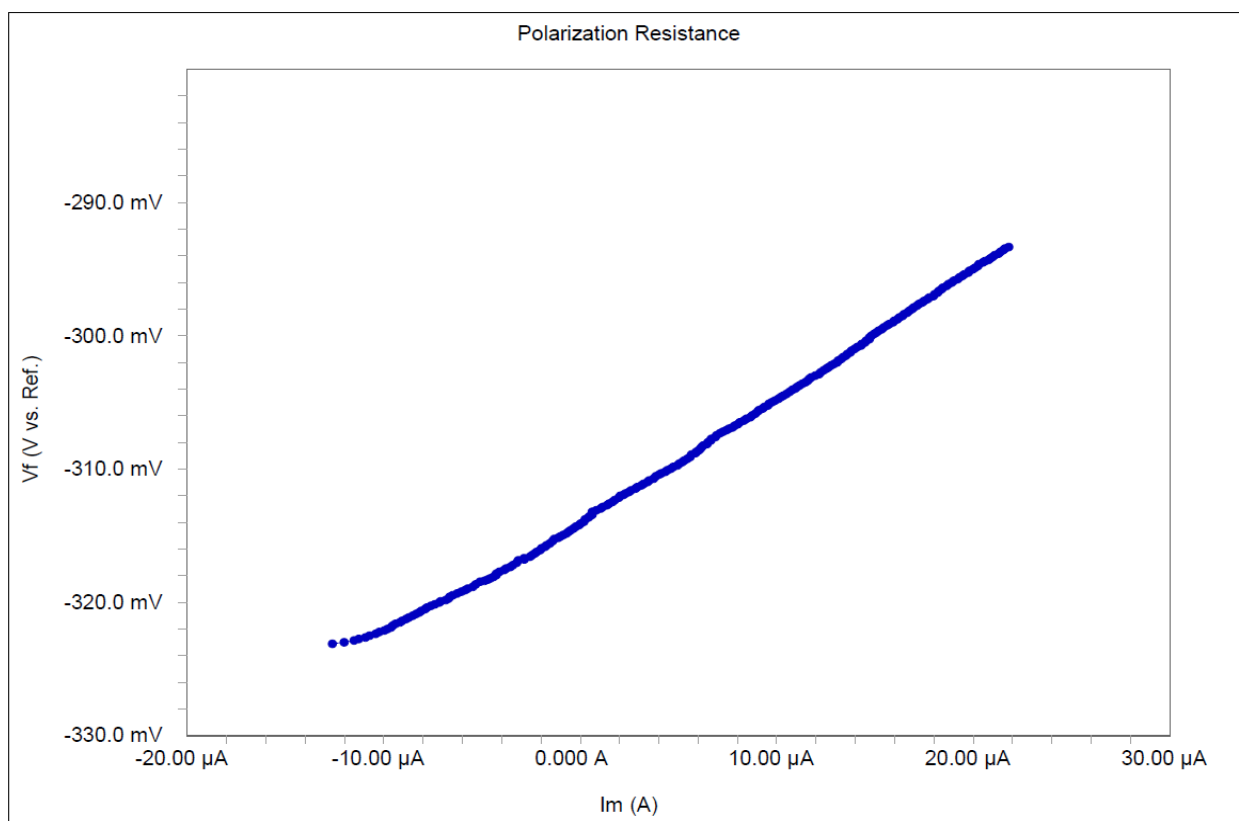


Figure 21 LPR data graph of GPC 1

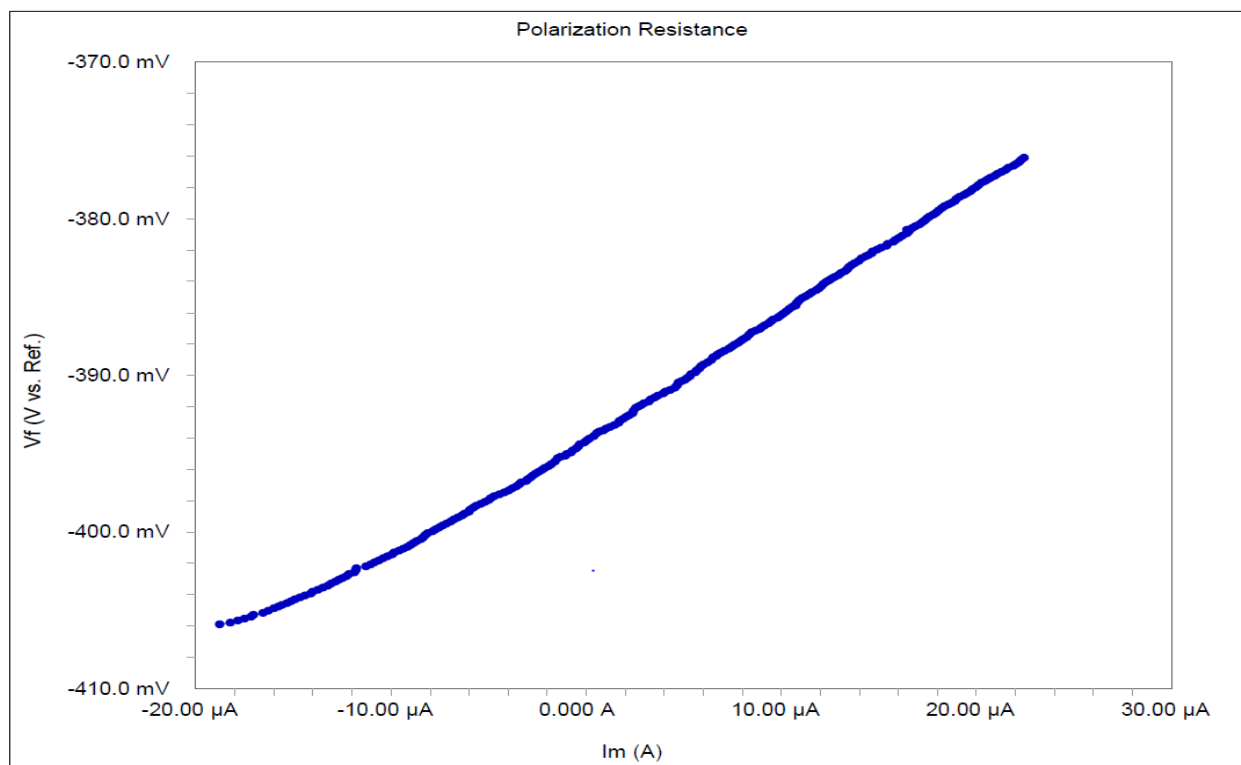


Figure 22 LPR data graph of GPC 2

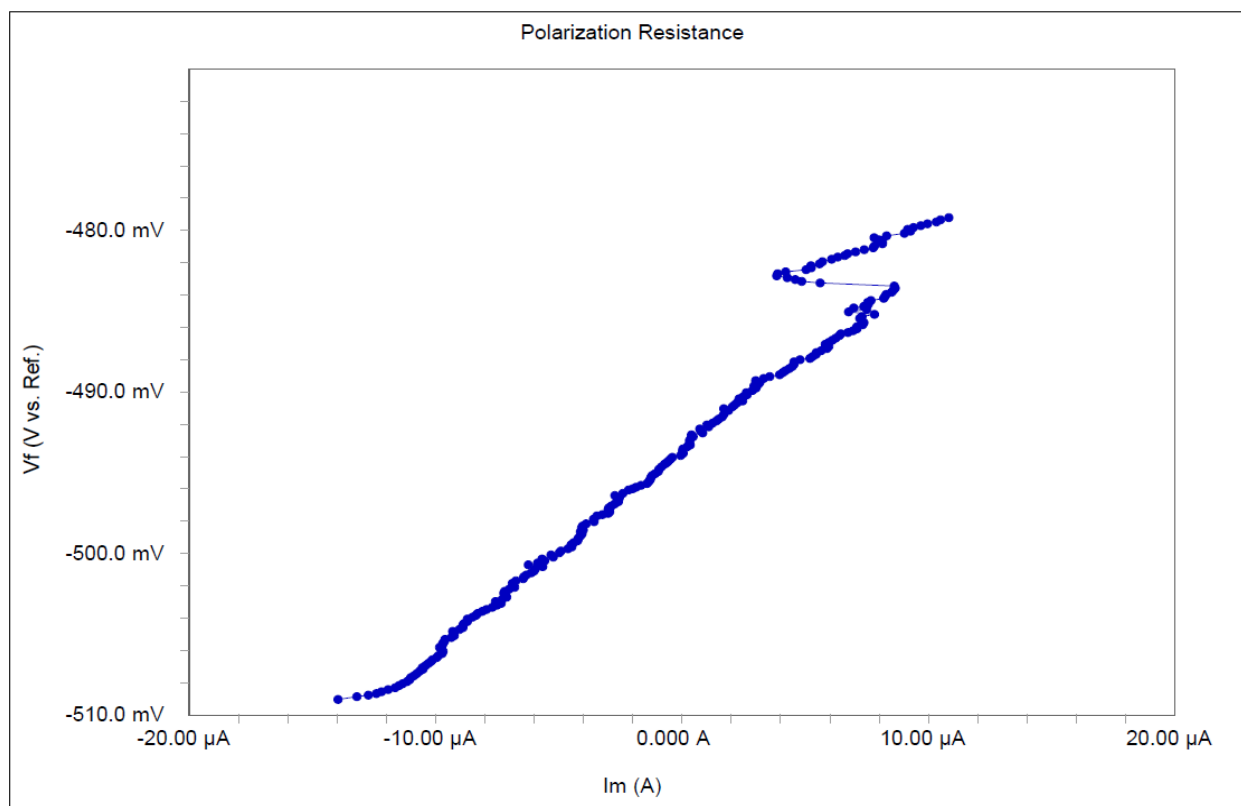


Figure 23 LPR data graph of GPC 3

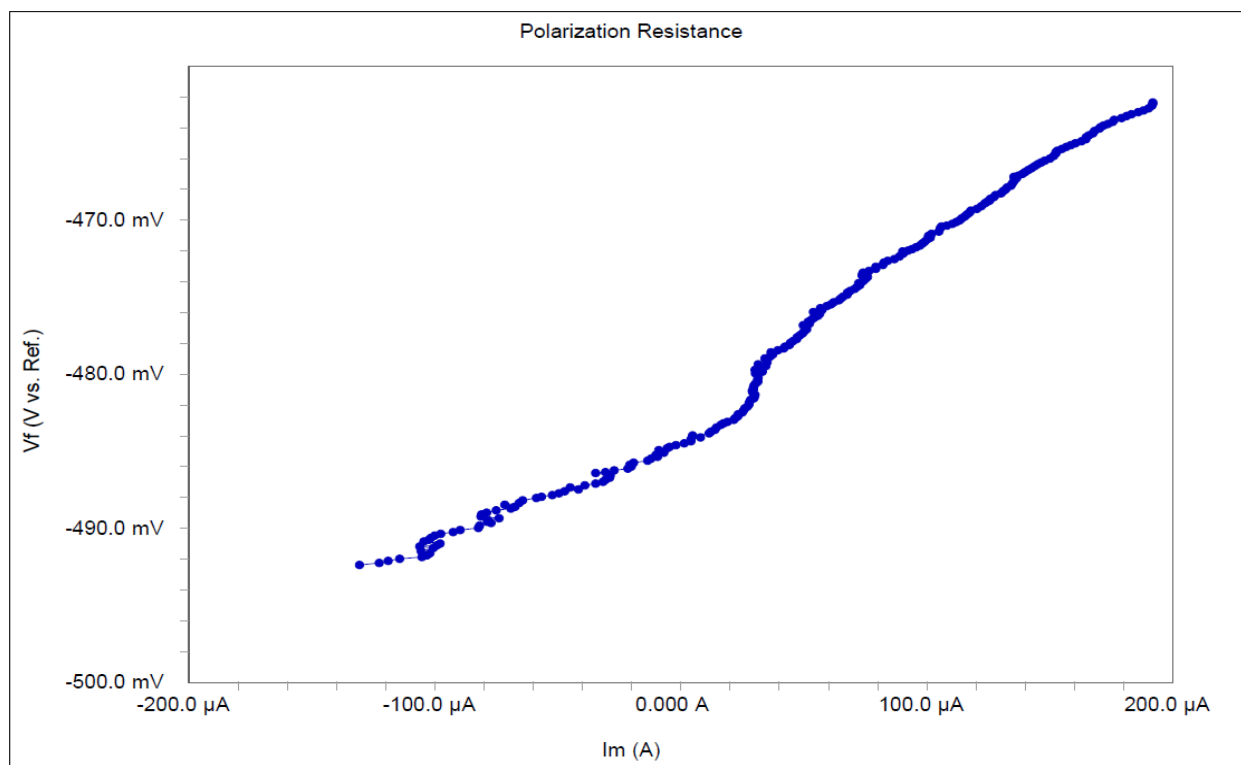


Figure 24 LPR data graph of OPC 1

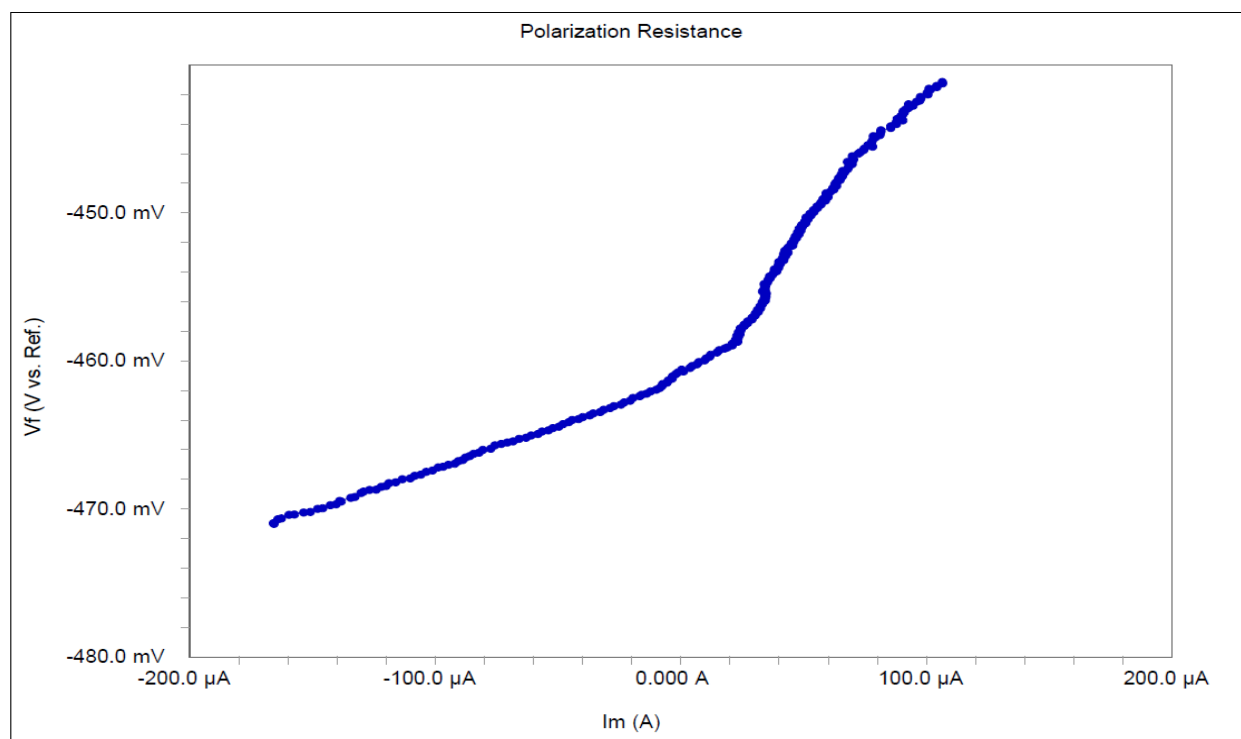


Figure 25 LPR data graph of OPC 2

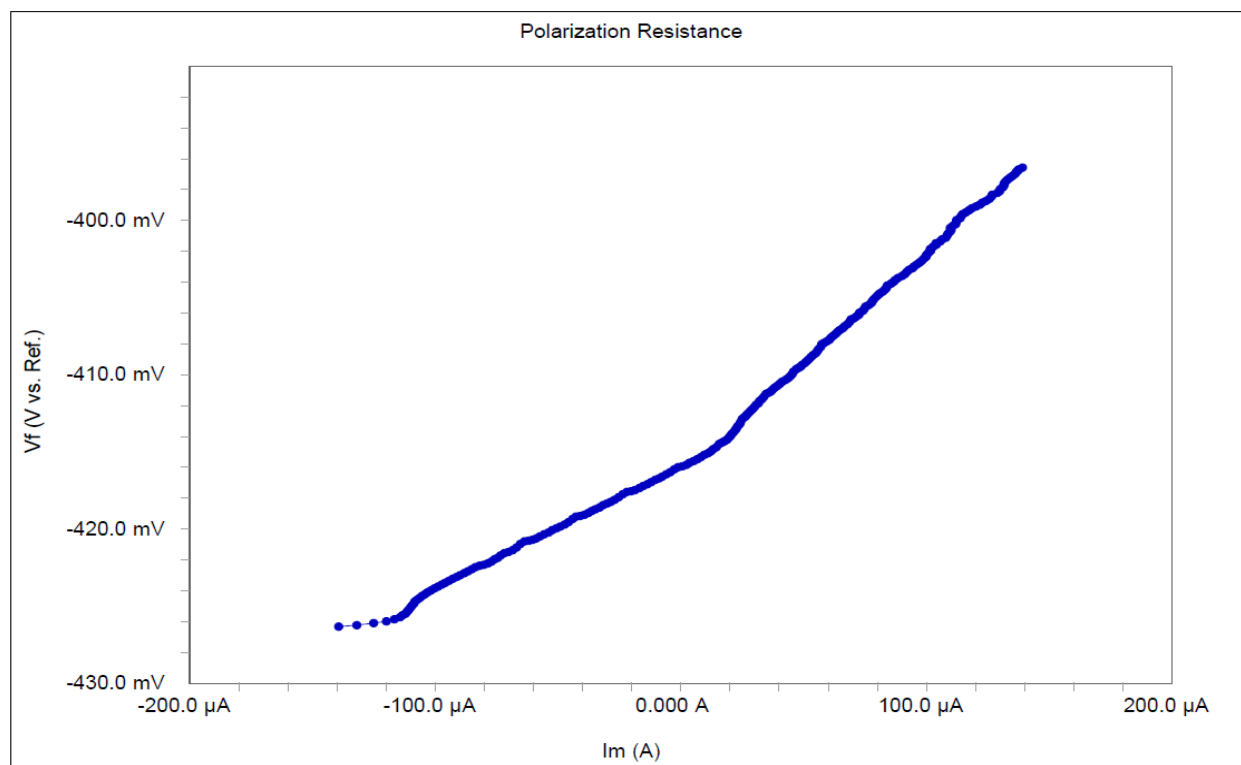


Figure 26 LPR data graph of OPC 3